energies

MDPI

Review

Research Progress on the Phase Change Materials for Cold Thermal Energy Storage

Xinghui Zhang [1], Qili Shi [1], Lingai Luo [2,*], Yilin Fan [2], Qian Wang [1] and Guanguan Jia [1]

[1] College of Civil Engineering, Taiyuan University of Technology, Taiyuan 030024, China; zxhtut@163.com (X.Z.); sqltyut@163.com (Q.S.); tyutwangqian@163.com (Q.W.); jgggjqx@126.com (G.J.)
[2] Université de Nantes, CNRS, Laboratoire de Thermique et Énergie de Nantes, LTeN, UMR6607, F-44000 Nantes, France; yilin.fan@univ-nantes.fr
* Correspondence: lingai.luo@univ-nantes.fr

Abstract: Thermal energy storage based on phase change materials (PCMs) can improve the efficiency of energy utilization by eliminating the mismatch between energy supply and demand. It has become a hot research topic in recent years, especially for cold thermal energy storage (CTES), such as free cooling of buildings, food transportation, electronic cooling, telecommunications cooling, etc. This paper summarizes the latest research progress of the PCMs-based CTES. Firstly, the classification of PCMs for low temperature storage is introduced; the thermal physical properties (e.g., phase change temperature (PCT) and latent heat) of suitable PCM candidates (−97 to 30 °C) for CTES are summarized as well. Secondly, the techniques proposed to enhance the thermal properties of PCMs are presented, including the addition of nanomaterials, the microencapsulation and the shape stabilization. Finally, several representative applications (−97 to 65 °C) of PCMs in different CTES systems are discussed. The present review provides a comprehensive summary, systematical analysis, and comparison for the PCMs-based CTES systems, which can be helpful for the future development in this field.

Keywords: cold thermal energy storage (CTES); phase change material (PCM); PCM performance; shape-stabilized PCM; cold application

Citation: Zhang, X.; Shi, Q.; Luo, L.; Fan, Y.; Wang, Q.; Jia, G. Research Progress on the Phase Change Materials for Cold Thermal Energy Storage. *Energies* **2021**, *14*, 8233. https://doi.org/10.3390/en14248233

Academic Editor: Chi-Ming Lai

Received: 28 September 2021
Accepted: 18 November 2021
Published: 7 December 2021

Highlights

- Latest research progress of PCM–CTES with a wide temperature range is reviewed.
- PCMs with a PCT range of (−100 to 30 °C) and the applications with a temperature range of (−97 to 65 °C) are covered.
- The potential and commercial PCMs and their thermophysical properties are presented.
- Technologies for enhancing the thermal properties of PCMs are introduced.
- Typical applications of PCMs for CTES are presented.

1. Introduction

Cold energy has a great demand in air conditioning of built environment, refrigeration, cold chain transportation, thermal management of electronic equipment, etc. Statistics show that refrigeration power consumption accounts for 15% of China's total power consumption, with an increase of 20% each year [1]. Facing this rapid growth, cold thermal energy storage (CTES) has attracted growing attention in recent years. It is one type of energy-saving technology, by storing the cooling capacity in one or some media at temperatures below the nominal temperature of the space or processing system, to be used during the period of peak cooling/cold demand. Common cold storage methods include sensible heat storage (SHS) and latent heat storage (LHS). In SHS, the cold is stored based on the sensible heat (temperature difference) of the storage medium. In LHS, cold is stored in the form of latent heat in materials undergoing phase transition, such as the fusion heat in solid–liquid phase transition. During melting, a large amount of cold is released

at an (almost) constant temperature for cooling purpose while during the solidification, the excessive cold can be stored. Figure 1 shows the general operation principle of the LHS.

The commonly used sensible cold storage medium is water, at a temperature of 5–12 °C for space cooling. The reasons for its popularity are due to its large specific heat capacity, simple equipment, low cost, and low technical requirements. However, water storage also suffers from several shortcomings, such as the low energy storage density, large volume of water tanks, and trouble in cold preservation and treatment. Ice and other phase change materials (PCMs) are commonly used as LHS. Compared with SHS, their cold storage capacity per unit volume is higher, reducing the area/volume of the storage equipment. As a relatively new medium for cold storage, PCM overcomes the disadvantages of large storage vessel volume and low efficiency of cooling devices based on chilled water storage, attracting extensive attention in recent years. However, the application of PCM for CTES purpose is still limited due to its low thermal conductivity. As a result, extensive research has been devoted to enhance its thermal performance by adding nanomaterials, microencapsulation, and shape-stabilization.

In terms of energy storage based on PCMs, most of the previous articles focused on heat storage while relatively little attention has been given to the cold storage. Except for scientific research papers, there are review articles on CTES using PCMs. For example, articles [2–8] reviewed the applications of PCMs in buildings. Dardir et al. [2] and Iten et al. [3] reviewed the applications of a PCM-to-air heat exchanger in free cooling of buildings, and the former focused on the applications under the condition of hot desert climate. Alizadeh and Sadrameli [4] presented the research of PCM in free cooling of residential and commercial buildings, with particular emphasis on updating the previous overview of modeling and simulation of TES integrating PCM into a building's passive cooling system. Souayfane et al. [5] mainly introduced the application of PCM to reduce building cooling load under different climatic conditions. Faraj et al. [6] introduced the heating, cooling, and hybrid applications of different PCMs in buildings (commercial and residential) from two aspects of passive and active systems. Akeiber et al. [7] and Romdhane et al. [8] mainly presented the application of PCM in building passive cooling. In the paper by Waqas and Din [9], the major challenges for the design of PCM-based cooling systems, including materials, thermophysical properties of PCMs, and packaging geometry, were discussed. Articles [10–13] reviewed the research status of PCMs from the perspective of materials. Li et al. [10] introduced PCMs with PCT in the range of 7–14 °C. Raj et al. [11] presented the PCMs used in building free cooling and the experimental work on heat transfer in free cooling. Sharma et al. [12] reviewed the research status of organic PCMs in energy storage. Kalnaes and Jelle [13] summarized commercial PCM products and presented their applications in buildings. Articles [14–17] reviewed the integration of PCMs in air conditioning systems. Zheng et al. [14] reviewed the working principle and characteristics of cold storage PCMs in solar air conditioning systems. Zhai et al. [15] presented the research on PCM–CTES devices and typical cold storage air conditioning systems. Osterman et al. [16] summarized the PCM-integrated cooling systems, including air conditioning and adsorption cooling systems. Gang et al. [17] introduced the latest development of cold storage PCM for air conditioning. Articles [18–20] reviewed the methods for improving the properties of PCMs. Sidik et al. [18] reviewed the research on the use of nanofluidic PCMs to enhance the thermal performance of CTESs using different base fluids. Ali [19] introduced systems that integrated heat pipe (HP) to improve the thermal performance of PCMs, and the applications of a hybrid system (based on HP–PCM) in energy storage and cooling systems. Kibria et al. [20] presented the experimental studies on the changes in the thermophysical properties of PCMs resulting from the dispersion of nanoparticles. Joybari et al. [21] reviewed the experimental work and research methods of the application of PCMs in household refrigerators. Selvnes et al. [22] focused on the research progress of applying PCM–CTES in refrigeration systems, including food transportation and packaging. Nie et al. [23] reviewed the methods of optimizing PCM performance, the modeling and experimental research of CTES device, and the applications

of cold storage in air conditioning and free cooling, mainly focusing on the applications of low-temperature energy storage.

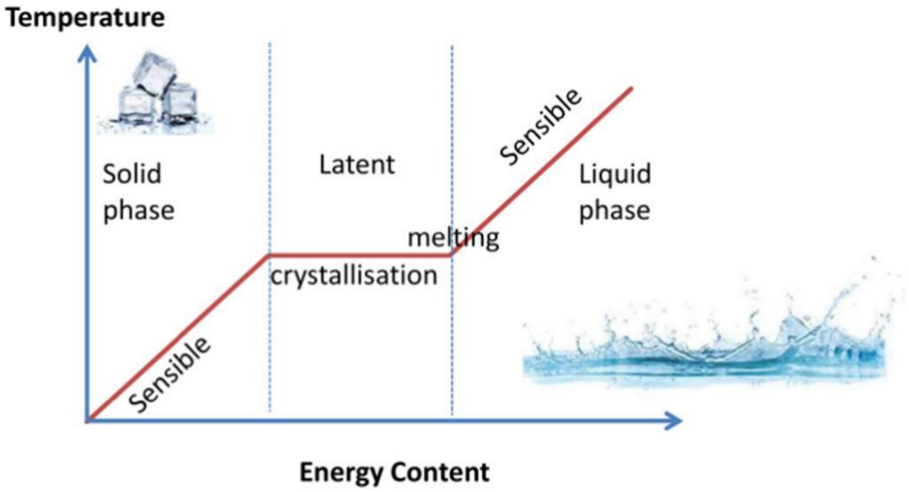

Figure 1. Basic principle of solid–liquid PCMs for energy storage. Reprinted with permission from ref. [18]. 28 September, 2021 Elsevier.

Relatively fewer review papers published in the literature on PCM for CTES cover different aspects such as materials, enhancement methods, and applications. For example, Oró et al. [24] reviewed comprehensive CTES applications using solid–liquid PCMs. Li et al. [25] summarized various kinds of suitable and promising PCMs for subzero cold storage applications with a special focus on their thermophysical properties. Recently, Yang et al. [26] comprehensively reviewed the research activities about CTES at subzero temperatures (from around −270 to below 0 °C) covering sensible, latent, and thermochemical technologies. Compared with these previous reviews, this paper covers a wide temperature range: materials from −100 to 30 °C and applications from −100 to 65 °C. At the same time, the topics addressed are also comprehensive and updated, covering materials, performance enhancement technologies, and applications in various fields. The rest parts of the article are organized as follows. Firstly, the PCMs suitable for different cold storage usages are classified based on their temperature ranges. Thermophysical properties such as phase change temperature (PCT), latent heat, and thermal conductivity, etc., which should be taken into account when selecting a suitable PCM, are provided. Then, the methods to enhance the thermal performance of PCMs are summarized, including adding nanomaterials, the microencapsulation, and the shape stabilization. The research methods and main achievements in recent years are listed to demonstrate the future research directions. Finally, the applications of PCMs in buildings, refrigeration, thermal management of electronic equipments, and other fields are introduced. In addition, suggestions on current challenges and future research directions are presented.

2. Phase Change Materials (PCMs)

Phase change material (PCM) is a kind of material that releases/absorbs thermal energy to provide useful heating/cooling effects during the phase transition. The working principle of solid–liquid PCMs is illustrated in Figure 1. Taking solid–liquid conversion as an example: cold is stored in the material during the phase transition from liquid to solid through the solidification process, or vice versa, cold release occurs during the melting process from solid to liquid. The most widely used PCMs for CTES can be classified into organic, inorganic, and eutectic PCMs. The classification of PCMs is shown in Figure 2.

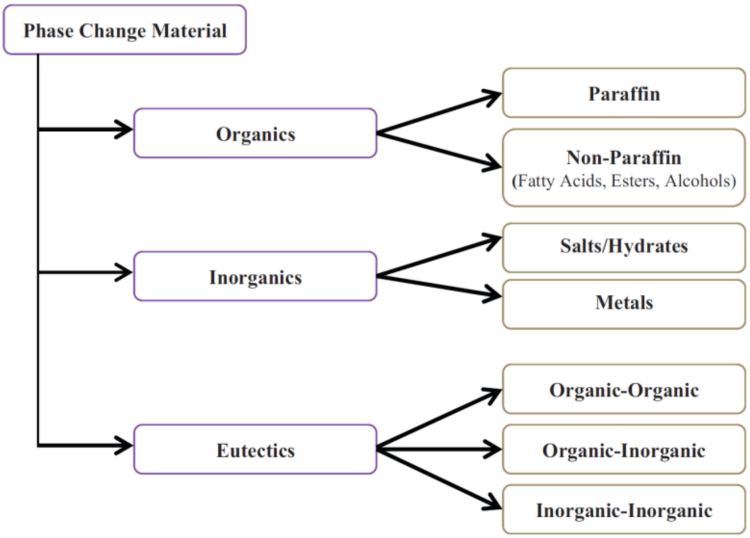

Figure 2. Classification of PCMs. Reprinted with permission from ref. [27]. 27 October 2021, Elsevier.

2.1. Organic PCMs for CTES

Organic PCMs are carbon-based compounds, mainly including paraffin-like materials such as alkanes, carboxylic acids, carboxylic lipids, polyols, n-alkane alcohols, sugar alcohols, and polyethers. The PCT of organic PCM is usually in the range 0–150 °C [28]. When the PCT is lower than 0 °C, the latent heat of organic PCM is relatively small, generally smaller than 200 kJ/kg [29]. Organic PCMs have the advantages of low subcooling, no phase separation, low corrosion, stable chemical properties, low cost, and good solid-state molding. The disadvantages are low thermal conductivity, relatively small latent heat, and low energy storage density. Moreover, the degradation phenomenon of phase change will appear with the increased number of charging–discharging cycles, restricting their service lifetime [30–32]. Table 1 provides some typical organic PCM candidates commonly used for CTES together with their physical properties.

Table 1. Typical organic PCMs for CTES.

Application Area	Material	PCT (°C)	Latent Heat (J/g)	Density (kg/m^3)	Thermal Conductivity (W/(m·K))	Specific Heat (kJ/(kg·K))	Reference
Space mission	Methanol	−97.15	99.25	904–810	0.210–0.206	2.20–2.40	[26]
	n-Hexane	−95.15	151.78	760–677	0.156–0.135	1.88–2.15	[26]
	Cyclopentane	−93.95	8.56	751	0.143	1.42–1.69	[26]
	Methylamine	−93.15	197.38	700	0.219	3.19–3.26	[26]
	n-Heptane	−90.55	140.12	774–700	0.156–0.138	1.96–2.15	[26]
	Ethane	−88.15	489.47	641–544	0.25–0.17	2.33–2.43	[26]
	Methylethylketone	−86.65	177.05	826	0.17–0.15	2.07–2.16	[26]
	Acetylene	−84.15	144.39	764.3–760.2	0.020	1.37	[26]
Low temperature cold storage/Low temperature logistics	n-Octane	−56.85	181.57	761–718	0.15–0.13	2.02–2.14	[26]
	2-Hexanone	−55.45	148.7	830	0.16–0.15	2.02–2.08	[26]
	3-Hexanone	−55.65	134.5	833	0.17–0.16	2.05–2.12	[26]
	n-Nonane	−53.65	117	773–734	0.15–0.13	1.99–2.12	[26]
	3-Heptanone	−37.1	153.5	822	0.15–0.14	-	[26]
	2-Heptanone	−35.0	172.6	851–834	0.15–0.14	-	[26]
	decane	−29.7	194.2	730	0.13110	2.22	[33]
	n-Dodecane	−12	216	745.64	0.134	2.039	[31]
	Diethylene glycol	−10~−7	247	1118	-	-	[31]
	n-Tridecane	−6	-	750.57	0.131	1.979	[31]

Table 1. *Cont.*

Application Area		Material	PCT (°C)	Latent Heat (J/g)	Density (kg/m^3)	Thermal Conductivity (W/(m·K))	Specific Heat (kJ/(kg·K))	Reference
Air conditioning	Food preservation	Tetrahydrofuran	5	280	-	-	-	[31]
		n-Tetradecane	5.5	226	765.78	0.129	2.031	[34]
		Formic Acid	7.8	247	1205.24	0.193	2.036	[34]
		Polyethylene glycol 400	8	99.6	1127	-	-	[34]
		Dimethyl adipate	9.7	164.6	1223	-	-	[31]
		n-Pentadecane	10.0	205	774.65	0.27	1.8	[35]
Building		Isopropyl palmitate	11	95–100	852	-	1.413	[36]
		Pelargonic	12.3	127	869.92	0.129	1.866	[34]
		Oleic Acid	13.5–16.3	-	890	-	-	[31]
		Isopropyl stearate	14–18	140–142	861	-	-	[36]
		Caprylic acid	16	150	1027.17	0.138	2.117	[36]
		Dimethyl sulfoxide	16.5	85.7	1097.19	0.161	1.700	[31]
		Acetic Acid	16.7	273	1050	-	-	[34]
		n-Hexadecane	18.2	238	774	0.21	2.001	[34]
		Propyl palmitate	16–19	186	864	-	-	[36]
		Polyethylene glycol 600	17–22	146	1130	-	-	[31]
		Glycerin	17.9	198.7	1291.14	0.222	1.506	[31]
		Butyl stearate	19	140–200	1097.39	0.156	1.492	[36]
		Lithium Chloride Ethanolate	21	188	-	-	-	[34]
		Dimethyl sebacate	21	120–135	986	-	-	[36]
		Octadecyl 3-mencaptopropylate	21	143	-	-	-	[36]
		n-Heptadecane	22	215	778	0.21	1.992	[34]
		Ethyl palmitate	23	122	870	-	-	[36]
		Myristic Acid + Capric	24	147.7	888	0.164	-	[34]
		Polyethylene Glycol 600	20–25	146	1100	-	-	[34]
	Thermal management of electronic equipment	Lauryl alcohol	25.83	215.83	890.92	0.144	2.322	[37]
		D-Lattic Acid	26	184	1249	-	-	[34]
		Octadecyl thioglyate	26	90	-	-	-	[36]
		Vinyl sterate	27–29	122	869	-	-	[36]
		n-Octadecane	28.2	245	775	0.149	1.964	[34]
		1-3 Methyl Pentacosane	29	197	-	-	-	[34]
		Methyl sterate	29	169	842.96	0.102	1.529	[36]
		Methyl Palmitate	29	205	860.10	0.140	2.139	[34]

2.2. Inorganic PCMs for CTES

Inorganic PCMs mainly contain hydrated salts and metals, with a PCT ranging between −100 and 1000 °C. Salt water complexes could be further classified according to three melting behaviors: homogeneous melting, heterogeneous melting, and semieutectic [38]. Metal PCMs include low melting point metals (e.g., Hg) and metal eutectic (e.g., 78.55 Ga–21.45 In [39]). Although metals have high volumetric melting enthalpy and high thermal conductivity, their application in TES is limited by their low melting enthalpy per unit weight [40]. Compared with organic PCMs, it shows the advantages of larger thermal conductivity and smaller degradation phenomenon. Disadvantages also exist, however, such as undercooling, phase separation, and corrosion to the packaging materials [15,30,41]. Table 2 shows the thermal properties of inorganic PCMs commonly used for CTES.

Table 2. Typical inorganic PCMs for cold energy storage.

Application	Material	PCT (°C)	Latent Heat (J/g)	Density (kg/m^3)	Thermal Conductivity (W/(m·K))	Specific Heat (kJ/(kg·K))	Reference
LNG cold energy recovery	Carbon Dioxide	−78.46	574	1562	0.011–0.015	0.78–0.83	[26]
Low temperature cold storage/low temperature logistics	Ammonia	−78.2	332.2	728–682	0.80–0.67	4.23–4.45	[26]
	Hg	−38.87	11.4	13,590	-	-	[31]
Household refrigerator/medical cold chain/high temperature cold storage/food preservation	H_2O	0.0	333	998.75	0.598	4.137	[34]
	$POCl_3$	1.0	85	1666.85	0.105	0.772	[34]
	D_2O	3.7	318	1104.42	0.595	4.19	[34]
	$SbCl_5$	4.0	33	2360	-	-	[34]
Air conditioning	$LiClO_4.3H_2O$	8	253	-	-	-	[34]
	$ZnCl_2.3H_20$	10	-	-	-	-	[36]
	H_2SO_4	10.4	100	1844.91	0.159	1.348	[34]
Building	$NH_4Cl.Na_2SO_4.10H_2O$	11	163	-	-	-	[34]
	$K_2HPO_4.6H_2O$	13	-	-	-	-	[36]
	lCl(β)	13.9	56	-	-	-	[34]
	$K_2HO_4.6H_2O$	14	108	-	-	-	[34]
	NaOH	16	200	1487.59	0.365	2.425	[36]
	MOF_6	17.0	50	2551	-	-	[34]
	$SO_3(\alpha)$	17.0	108	1853.026	0.131	1.398	[34]
	lCl(α)	17.2	69	-	-	-	[34]
	$NaCl.Na_2SO_4.10H_2O$	18	286	-	-	-	[34]
	$Na_2CrO4.10H_2O$	18	-	-	-	-	[36]
	$KF.4H_2O$	18	330	-	-	-	[34]
	$K_2HPO_4.4H_2O$	18.5	231	1447	-	-	[34]
	$Na_2SO_4.10H_2O$	21	198	-	-	-	[36]
	$FeBr_3.6H_2O$	21	105	-	-	-	[36]
	P_4O_6	23.7	64	-	-	-	[34]
Thermal management of electronic equipment	$Mn(NO_3)_2.6H_2O$	25	148	1738	-	-	[34]
	$LiBO_2.8H_2O$	25.7	289	-	-	-	[34]
	H_3PO_4	26.0	147	-	-	-	[34]
	$FeBr_3.6H_2O$	27	105	-	-	-	[34]
	Cs	28.3	15	1870	-	-	[34]
	$CaCl_2.6H_2O$	29–30	170–192	1562	0.561	-	[34]
	$CaCl_2.12H_2O$	29.8	174	-	-	-	[36]
	Ga	30.0	80	1550	-	-	[34]
	$AsBr_3$	30.0	38	-	-	-	[34]
	$LiNO_3.3H_2O$	30	189/296	-	-	-	[34]
	$LiNO_3.2H_2O$	30	296	-	-	-	[36]

2.3. Eutectic PCMs for CTES

Eutectic PCMs refer to crystal mixtures formed by two or more kinds of low-melting components in the crystallization process, including organic–organic, organic–inorganic, and inorganic–inorganic mixtures [42]. This type of PCM forms a crystal mixture during solidification and does not separate during melting [43]. The main advantage of eutectic PCMs is that the PCT can be controlled by adjusting the proportion of the components, opening a wide prospect for different applications. Other advantages of eutectic PCMs include high thermal conductivity, high density, no phase separation, and no subcooling. Nevertheless, the latent heat and specific heat are usually lower than those of alkane and inorganic PCMs [15,30,44]. Tables 3 and 4 list some organic and inorganic eutectic PCMs tested in the literature and their thermal properties.

Table 3. Typical organic eutectic PCMs for CTES.

Materials	PCT (°C)	Latent Heat (J/g)	Density (kg/m^3)	Thermal Conductivity (W/(m·K))	Specific Heat (kJ/(kg·K))	Reference
Polyethylene glycol 200/Polyethylene glycol 300 (4:96 wt%)	−20	-	-	-	-	[26]
Dodecane + Tridecane (82.3:17.7 by mole)	Tm −16~−12/Tf −17~−15	Hm 185/Hf 165	-	-	-	[45]
Polyethylene glycol 200/Polyethylene glycol 300 (20:80 wt%)	−15	-	-	-	-	[26]
Polyethylene glycol 200/Polyethylene glycol 300 (30:70 wt%)	−10	-	-	-	-	[26]
Dodecane + Tridecane (60:40 by volume)	−9.7	159	-	-	-	[31]
Dodecane + Tridecane (50:50 by volume)	−9.1	145	-	-	-	[31]
Dodecane + Tridecane (40:60 by volume)	−8	147	-	-	-	[31]
Dodecane + Tridecane (20:80 by volume)	−5.4	126	-	-	-	[31]
Tridecane + Tetradecane (80:20 by volume)	−1.5	110	-	-	-	[31]
Tridecane + Tetradecane (60:40 by volume)	−0.5	138	-	-	-	[31]
Tridecane + Tetradecane (40:60 by volume)	0.7	148	-	-	-	[31]
N-decanoic acid + N-decanol (36:64 by mole)	1.2	177.74	-	-	-	[46]
Hexadecane + Tetradecane	1.7–17.9	146–227	-	-	-	[47]
Dodecanol + Octanoic acids (40:60 by mass)	2.08	224.5	-	0.3	-	[48]
Tridecane + Tetradecane (20:80 by volume)	2.6	212	-	-	-	[31]
N-decanoic acid + Methyl laurate (30:70 by mole)	3.2	188.10	-	-	-	[46]
Caprylic acid + Lauric acid (9:1 by mole)	3.77	151.5	-	-	-	[49]
Lauric acid + Tetradecane (21:79 by mole)	4.2	206.17	-	-	-	[46]
Tetra decane + Lauryl alcohol (66:34)	4.3	241.7		0.2737		[50]
Tetra decane + Lauryl alcohol (66:34) + EG	4.3	245.1	-	0.9657		[50]
Tetradecane + Hexadecane (50:50 by volume)	4.9	154.839	-	-	-	[51]
Paraffin C14 + C15 + C16 + C17 + C18 (33.4:47.3:16.3:2.6:0.4)	5.2	158.3	-	-	-	[51]
Dodecanol + Octanoic acid (2:3 by mass)	6.2	173.2	-	-	–	[52]

Table 3. *Cont.*

Materials	PCT (°C)	Latent Heat (J/g)	Density (kg/m^3)	Thermal Conductivity (W/(m·K))	Specific Heat (kJ/(kg·K))	Reference
Caprylic acid + 1-dodecanol (70:30)	6.52	171.06	-	-	-	[53]
Caprylic acid + Palmitic acid (90:10)	Tm 6.54/Tf 4.31	ΔHm 116.477/ΔHf 116.235	-	-	-	[54]
Caprylic alcohol + Mynstyl alcohol (73.7:26.3 by mass)	6.9	169.1	-	0.1739	-	[55]
Lauryl alcohol + Octanoic acids (40.6:59.4)	7	178.6	-	-		[56]
Oleic + Capric acid (37:63 by mole)	10	60		Liquid: 0.194/solid: 0.201	-	[57]
Capric acid and lauric acid (65:35 by mole) + Pentadecane (50:50 by volume)	10.2	157.8	Liquid: 827.8/solid: 850.4	-	Liquid: 2.89/solid: 2.44	[58]
Capric acid and lauric acid (65:35 by mole) + Pentadecane (70:30 by volume)	11.3	149.2	Liquid: 858/solid: 872.7	-	Liquid: 2.57/solid: 2.27	[58]
$C_5H_5C_6H_5$ + $(C_6H_5)_2O$ (26:73.5)	12	97.9				[34]
Capric acid and lauric acid (65:35 by mole) + 0.10 mol Cineole	12.3	111.6	927	-	Liquid: 2.37/solid: 1.71	[59]
Capric acid and lauric acid (65:35 by mole) + 0.10 mol Methyl Salicylate	12.5	126.7	Liquid: 1182/solid: 1272.9	-	Liquid: 2.41/solid: 1.92	[59]
Capric acid and lauric acid (65:35 by mole) + Pentadecane (90:10 by volume)	13.3	142.2	Liquid: 883.2/solid: 891.3	-	Liquid: 2.42/solid: 872.72.08	[58]
Capric acid and lauric acid (65:35 by mole) + 0.10 mol Eugenol	13.9	117.8	1091	-	Liquid: 2.63/solid: 2.01	[59]
Capric acid + Lauric acid-oleic acid	Tm 14.5/Tf 10.5	109.2	Liquid: 839.7/solid: 845.1	Liquid: 0.141/solid: 0.145	Liquid: 2.214/solid: 1.825	[60]
Lauric + 1-dodecanol (29:71)	17	175.3	-	0.180	-	[61]
Capric acid + Lauric aci (65:35 by mole)	18	140.8	Liquid: 894.9/solid: 900.0	Liquid: 0.139/solid: 0.143	Liquid: 2.24/solid: 1.97	[59]
Myristic + 1-dodecanol (17:83)	18.43	180.8	-	0.180	-	[61]
Lauryl alcohol + Cetyl alcohol (80:20)	20.01	191.63	-	0.1–0.2	-	[62]
Palmitic + 1-dodecanol (10:90)	20.08	191	-	0.180	-	[61]
Capric acid + Myristic acid (85:15 by mass)	20.86	156.99	-	0.152	-	[63]
Dodecanol + Stearic acid (82:18 by mass)	21.3	205.9	-	-	-	[64]
Lauric acid + Myristyl alcohol (40:60)	Tm 21.3/Tf 19.9	ΔHm 151.1/ΔHf 151.6	-	-	-	[65]
Capric acid + Palmitic acid (76.5:23.5)	Tm 21.85/Tf 22.15	ΔHm 171.22/ΔHf 173.16	-	-	-	[66]

Table 3. *Cont.*

Materials	PCT (°C)	Latent Heat (J/g)	Density (kg/m^3)	Thermal Conductivity (W/(m·K))	Specific Heat (kJ/(kg·K))	Reference
Capric acid + Cetyl alcohol (70:30)	Tm 22.89/Tf 11.97	ΔHm 144.92/ΔHf 145.85	-	-	-	[67]
Lauryl alcohol + Stearyl alcohol (90:10)	22.93	205.79				[37]
Dodecyl Acetate + Amyl valerate (34:66)	24	147.7				[34]
Eicosane + Capric acid (25:75)	24.96	200.3	-	-	-	[68]
Lauric acid + 1-tetradecanol (40:60)	24.33	161.45	-	-	40 °C: 2.3635/10 °C: 2.1635	[69]
Methyl palmitate + Lauric acid (60:40)	Tm 25.6/Tf 20.2	ΔHm 205.4/ΔHf 205.8	Liquid: 840.6/solid: 887.7	0.1802	Liquid: 1.952/solid: 1.513	[69]
Stearic acid + N-octadecane (4:96)	27.4	227	-	-	-	[70]

Table 4. Typical inorganic salt solution and eutectic PCMs for CTES.

Materials	PCT (°C)	Latent Heat (J/g)	Reference
24.8 wt% HCl	−86	73.77	[24]
24 wt% LiCl	−67	36.26	[24]
$ZnCl_2$ aqueous solution (51%)	−62	116.84	[71]
$FeCl_3$ aqueous solution (33.1%)	−55	155.52	[71]
$CaCl_2$ aqueous solution (29.8%)	−55	164.93	[71]
30.5 wt% $CaCl_2$	−49.5	76.81	[24]
$CuCl_2$ aqueous solution (29.8%)	−40	166.17	[71]
K_2CO_3 aqueous solution (39.6%)	−36.5	165.36	[71]
21.01 wt% $MgCl_2$	−33.5	36.30	[24]
$MgCl_2$ aqueous solution (17.1%)	−33.6	221.86	[71]
$Al(NO_3)_3$ aqueous solution (30.5%)	−30.6	207.63	[71]
$Mg(NO_3)_2$ aqueous solution (34.6%)	−29	186.93	[71]
$Zn(NO_3)_2$ aqueous solution (39.4%)	−29	169.88	[71]
NH_4F aqueous solution (32.3%)	−28.1	187.83	[71]
NaBr aqueous solution (40.3%)	−28	175.69	[71]
27.9 wt% NaCl	−23	26.10	[15]
KF aqueous solution (21.5%)	−21.6	227.13	[71]
NaCl aqueous solution (22.4%)	−21.2	228.14	[71]
Aqueous sodium chloride (23.3 wt%) at eutectic composition	−21.1	246.6	[33]
$MgCl_2$ aqueous solution (25%)	−19.4	223.10	[71]
$(NH_4)_2SO_4$ aqueous solution (39.7%)	−18.5	187.75	[71]
$NaNO_3$ aqueous solution (36.9%)	−17.7	187.79	[71]
NH_4NO_3 aqueous solution (41.2%)	−17.35	186.29	[71]
$Ca(NO_3)_2$ aqueous solution (35%)	−16	199.35	[71]
NH_4Cl aqueous solution (19.5%)	−16	248.44	[71]
K_2HPO_4 aqueous solution (36.8%)	−13.5	197.79	[71]
$Na_2S_2O_3$ aqueous solution (30%)	−11	219.86	[71]
KCl aqueous solution (19.5%)	−10.7	253.18	[71]
$MnSO_3$ aqueous solution (32.2%)	−10.5	213.07	[71]
NaH_2PO_4 aqueous solution (23.4%)	−9.9	214.25	[71]
$BaCl_2$ aqueous solution (22.5%)	−7.8	246.44	[71]
22.1 wt% $BaCl_2$	−7.7	10.2	[24]
$ZnSO_3$ aqueous solution (27.2%)	−6.5	235.75	[71]

Table 4. *Cont.*

Materials	PCT (°C)	Latent Heat (J/g)	Reference
$Sr(NO_3)_2$ aqueous solution (24.5%)	−5.75	243.15	[71]
$KHCO_3$ aqueous solution (16.95%)	−5.4	268.54	[71]
18.63 wt% $MgSO_4$	−4.8	84.96	[24]
$NiSO_4$ aqueous solution (20.6%)	−4.15	258.61	[71]
$MgSO_4$ aqueous solution (19%)	−3.9	264.42	[71]
Na_2SO_4 aqueous solution (12.7%)	−3.55	284.95	[71]
NaF aqueous solution (3.9%)	−3.5	314.09	[71]
KNO_3 aqueous solution (9.7%)	−2.8	296.02	[71]
Na_2CO_3 aqueous solution (5.9%)	−2.1	310.23	[71]
$FeSO_4$ aqueous solution (13%)	−1.8	286.81	[71]
$CuSO_4$ aqueous solution (11.9%)	−1.6	290.91	[71]
4.03 wt% Na_2SO_4	−1.2	1.07	[15]
31% Na_2SO_4 + 13% NaCl + 16% KCl + 40% H_2O	4	234	[34]
Tetrabutyl ammonium bromide aqueous solutio (15%)	6.6	-	[72]
Tetrabutyl ammonium bromide aqueous soluti (40%)	9	ΔHm 187.867/ΔHf 137.799	[73]
$Na_2SO_4{\cdot}10H_2O$ + NH_4Cl + KCl + K_2SO_4 + Carboxymethyl cellulose + $(NaPO_3)_6$ + borax + boric acid (76 + 10.3 + 3.6 + 2 + 3.2 + 0.1 + 2.4 + 2.4)	Tm 9.3/Tf 8.25	114.37	[74]
32% Na_2SO_4 + 14% NaCl + 12% NH_4Cl + 42% H_2O	11	-	[34]
Tetrabutyl ammonium bromide aqueous solution (45%)	12.5	-	[72]
55% $CaCl_2{\cdot}6H_2O$ + 55% $CaBr_2{\cdot}6H_2O$	14.7	140	[28]
$NaOH{\cdot}(3/2)H_2O$	15	-	[28]
$Mn(NO_3){\cdot}6H_2O$ + $MgCl_2{\cdot}6H_2O$	15–25	125.9	[28]
45–52% $LiNO_3{\cdot}3H_2O$ + 48–55% $Zn(NO_3)_2{\cdot}6H_2O$	17.2	220	[28]
37% Na_2SO_4 + 17% NaCl + 46% H_2O	18	-	[34]
25% Na_2S_4 + 21% $MgSO_4$ + 54% H_2O	21–24	-	[34]
$LiNO_3{\cdot}3H_2O$ + $Ni(NO_3)_2$ (55–65:35–45)	24.2	230	[28]
$Ca(NO_3)_2{\cdot}6H_2O$ + $Zn(NO_3)_2{\cdot}6H_2O$ (45:55)	25	130	[28]
$CaCl_2{\cdot}6H_2O$ + $MgCl_2{\cdot}6H_2O$ (66.6:33.3)	25	127	[28]
50% $CaCl_2$ + 50% $MgCl_2$ + $6H_2O$	25	95	[28]
$CaCl_2$ + NaCl + KCl + H_2O (48:4.3:0.4:47.3)	27	188	[28]
$Ca(NO)_3.4H_2O$ + $Mg(NO)_3.6H_2O$ (47:53)	30	136	[34]

2.4. Commercial PCMs

In addition to the abovementioned PCMs that are generally in the research stage, some PCMs have been developed and are commercially available on the market. Table 5 lists some commercial PCMs and their thermal performance; it can be seen that currently commercially available PCMs are mainly salt solutions and paraffin.

Table 5. Typical commercialized PCMs for CTES.

Composition	Type	PCT (°C)	Latent Heat (J/g)	Source	Reference
E-90	Eutectic solutions	−90	90	PCM Products Ltd.	[75]
E-78	Eutectic solutions	−78	115	PCM Products Ltd.	[75]
E-75	Eutectic solutions	−75	102	PCM Products Ltd.	[75]
E-65	Eutectic solutions	−65	240	PCM Products Ltd.	[75]
E-62	Eutectic solutions	−62	180	PCM Products Ltd.	[75]
E-60	Eutectic solutions	−60	172	PCM Products Ltd.	[75]
SN 50	Inorganic salt solution	−50	325	TEAP	[76]
SN 33	Inorganic salt solution	−33	245	Cristopia	[77]
TH 31	Salt hydrate	−31	131	TEAP	[76]
MPCM (−30)	Paraffin	−30	140–150	Microtek Laboratories, Inc.	[78]
SN 29	Inorganic salt solution	−29	233	Cristopia	[77]
SN 26	Inorganic salt solution	−26	168	Cristopia	[77]
TH 23	Salt hydrate	−23	230	TEAP	[76]
TH 21	Salt hydrate	−21	222	TEAP	[76]
SN 21	Inorganic salt solution	−21	240	Cristopia	[77]
STL 21	Inorganic salt solution	−21	240	Mitsubishi Chemical	[79]
ClimSel C-18	Inorganic salt solution	−18	306	Climator	[80]
SN 18	Inorganic salt solution	−18	268	Cristopia	[77]
STL 16	Inorganic salt solution	−16	289	Mitsubishi Chemical	[79]
TH 16	Salt hydrate	−16	289	TEAP	[76]
AN 15	Inorganic salt solution	−15	311	Cristopia	[77]
AN 12	Inorganic salt solution	−12	306	Cristopia	[77]
STLN 10	Inorganic salt solution	−11	271	Mitsubishi Chemical	[79]
AN 10	Inorganic salt solution	−10	310	Cristopia	[77]
TH 10	Inorganic salt solution	−10	283	TEAP	[76]
MPCM (−10)	Paraffin	−9.5	150–170	Microtek Laboratories, Inc.	[78]
STL-6	Inorganic salt solution	−6	284	Mitsubishi Chemical	[79]
TH-4	Inorganic salt solution	−4	386	TEAP	[76]
RT-4	Paraffin	−4	179	Rubitherm GmbH	[81]
SLT 3	Inorganic salt solution	−3	328	Mitsubishi Chemical	[79]
AN 3	Inorganic salt solution	−3	328	Cristopia	[77]
RT3	Paraffin	3	198	Rubitherm GmbH	[81]
RT4	Paraffin	4	182	Rubitherm GmbH	[81]
RT5	Paraffin	5.2	158.3	Rubitherm GmbH	[81]
RT6	Paraffin	6	175	Rubitherm GmbH	[81]
MPCM (6)	Paraffin	6	157–167	Microtek Laboratories, Inc.	[78]
ClimSel C7	Organic	7	130	Climator AB	[80]
PureTemp 8	Organic	8	180	PureTemp	[82]
PCM-OM08P	Organic	8	190	SAVENR	-
A8	Organic	8	150	EPS Ltd.	[83]
RT 8	Organic	8	180	Rubitherm	[81]
RT 9	Organic	9	160	Rubitherm	[81]
A9	Organic	9	140	EPS Ltd.	[83]
RT10	Organic	10	150	Rubitherm	[81]
RT 10 HC	Organic	10	195	Rubitherm	[81]
S1 0	Organic	10	155	Cristopia	[77]
PCM-OM11P	Organic	11	260	SAVENR	-
PureTemp 12	Organic	12	185	PureTemp	[82]
RT12	Organic	12	150	Rubitherm	[81]
ClimSel C15	Salt solution	15	130	Climator AB	[80]
E17	Inorganic salt solution	17	143	-	[31]
E19	Inorganic salt solution	19	146	-	[31]
RT20	Paraffin	20	140	Rubitherm	[31]
Emerest 2325	Fatty acid	20	134	-	[31]
Emerest 2326	Fatty acid	20	139	-	[31]
FMC	Paraffin	20–23	130	-	[31]

3. Enhancement of PCMs Performance

The low thermal conductivity, liquid leakage in solid–liquid phase transition, and supercooling of PCMs can cause the poor thermal performance and cycling instability of CTES. In order to optimize the performance of PCMs, a number of approaches have been adopted, including the addition of nanomaterials, the encapsulation and the shape stabilization.

3.1. Addition of Nanomaterials

Nanomaterials (such as metal particles, carbon fiber, graphite, and nanoparticle composites) with high thermal conductivity have been added to conventional PCMs [84]. The selection of appropriate nanoparticles is critical in augmenting the charging/discharging rates [15]. Table 6 shows some typical cases of nanomaterial addition to increase the thermal conductivity of PCMs.

Jia et al. [85] took 5% sorbitol aqueous solution as the base fluid (SH95), with a PCT of −2.9 °C, a latent heat enthalpy of 302.5 kJ/kg, and an undercooling degree of 7.9 °C. Al_2O_3, Fe_2O_3, and TiO_2 nanofluid solutions of 0.10%, 0.20%, 0.30%, 0.40%, and 0.50% were prepared. Their experimental results showed that these nanomaterials all have the effect of reducing the undercooling degree of SH95. When the mass fraction of nanofluid TiO_2 was 0.50%, the undercooling degree was 1.4 °C, and the reduction range was up to 82.5% (best effect). The thermal conductivity enhancement effects of the tested nanoparticles were: TiO_2 > Al_2O_3 > Fe_2O_3, reaching 0.612, 0.609, and 0.597 W/(m·K), respectively. No phase separation of the SH95 was found after 50 cycles of operation when 1.0% sodium polyacrylate (PAAS) was added to prevent nanomaterial precipitation from affecting the material properties. However, the PCT of SH95A decreased by 0.8 °C and the latent enthalpy decreased by 13.4% after 100 cycles.

Zhang et al. [86] took positive octylic acid (OA)–lauric acid (LA) binary PCMs with a mass ratio of 81:19 as the base fluid. The PCT of the base fluid was 4.5 °C, the latent heat was 138.4 J/g, and the thermal conductivity was 0.2969 W/(m·K). Nanocomposite PCMs were prepared by adding hydroxylated multiwall carbon nanotubes (MWCNT-OH), Fe_2O_3, Al_2O_3, Cu, and dispersant SDBS using the ultrasonic oscillation method. It was found that with MWCNT-OH mass concentration of 0.10 g/L, the thermal conductivity of the composite was 0.3691 W/(m·K), 21.9% higher than the base fluid. The latent heat increased by 2.9% and the charging time was shortened by 16.7%. The results of cyclic stability test showed that the phase separation did not occur after 200 cycles, indicating good stability of the nano-enhanced PCMs.

Liu et al. [87,88] took $BaCl_2$-H_2O eutectic salt solution (22.5 wt%) as the base fluid. The PCT of the base fluid was −8.4 °C, the latent heat was 281.1 kJ/kg, the thermal conductivity was 0.56 W/(m °C), and the undercooling was 3.78 °C. Nano TiO_2 particles (20 nm) with different volume fractions (0.167%, 0.283%, 0.565%, and 1.130%) were added into the base fluid. It was found that the thermal conductivity of TiO_2-$BaCl_2$-H_2O nanocomposite materials could be significantly improved at 25 °C. When the volume fraction of nanoparticles was 1.13%, the thermal conductivity of nanocomposites could reach the maximum, 16.74% higher than that of $BaCl_2$-H_2O solution at the same temperature. At −5 °C, the thermal conductivity of nanocomposites can be increased by 12.76%, indicating good heat transfer enhancement at lower temperatures. The undercooling could also be basically eliminated. After 50 ice storage/release operation cycles, the latent heat and PCT remained basically unchanged.

Sathishkumar et al. [89] used deionized water as the base fluid. Dodecane with mass fraction of 0.25% and sodium dobecyl benzene sulfonate (SDBS) as surfactant were added to the base fluid, and graphene carbon nanoplates (GNPs) with mass concentrations of 0.3%, 0.6%, 0.9%, and 1.2% were added to prepare nanofluid PCMs (NFPCM). The measurements showed that the thermal conductivities of NFPCMs all increased proportionally to the concentration of GNPs; the maximum thermal conductivity enhancement of NFPCMs containing 1.2 wt% GNPs were 56% (solid state) and 11.7% (liquid state) between −10 and 40 °C. The increase of GNPs significantly reduced the water supercooling from −7 °C to −2.5 °C, accompanied by a 25% reduction in the solidification time owing to their high thermal conductivity and large surface-to-volume ratio of GNPs.

Table 6. Typical cases of adding nanomaterials to enhance the thermal conductivity of PCM.

PCM	Nanomaterials	PCT of Composites (°C)	Latent Heat of Composites (J/g)	Thermal Conductivity of Composites (W/(m·K))	Improvement Rate of Thermal Conductivity	Application	Year	Reference
Sorbitol aqueous solution (5 wt%)	0.40 wt% TiO_2	−2.9 (no change)	293.8 (decreased by 2.9%)	0.62	29.1%	Cold chain transportation	2019	[85]
N-octanoic acid + Lauric acid (81:19 by mass)	0.1 g/L Hydroxylated multi walled carbon nanotubes	4.5 (no change)	142.4 (increased by 2.9%)	0.36	21.9%	Cold chain transportation	2019	[86]
$BaCl_2$ aqueous solution (22.5 wt%)	TiO_2 with volume fraction of 1.13%	−8.5 (no change)	254.2 (decreased by 9.57%)	0.67	16.74%	Refrigeration station of beer industry	2015, 2005	[87,88]
Organic PCM for air conditioning	0.4 g/L Multi walled carbon nanotubes	-	-	0.2436	21.9%	Air conditioning	2012	[90]
Organic PCM for air conditioning	TiO_2 nanoparticles	-	-	0.519	22%	Air conditioning	2008, 2004	[91,92]
Paraffin RT4	5% Carbon nanotubes	No change	128.2 (decreased by 15.5%)	0.486	38%	-	2017	[93]
Deionized water	1.2 wt% Graphene nanoplatelets	−2.5	-	3.198 (solid state)/0.6702 (liquid state)	56% (solid state)/11.7% (liquid state)	Building cooling	2016	[89]
Commercialized paraffin wax	40 wt% Hexagonal boron nitride nanosheets	-	80.17 (decreased by 12%)	3.47	12 times	Thermal management of electronic equipment	2016	[94]
Oleic and capric acid eutectic	0.1 wt% Porous activated carbon nanosheets	-	52.7 (decreased by 12%)	0.3007	55%	Banana ripening cold storage	2017	[57]
Ethylene glycol aqueous solution	0.5% Multi walled carbon nanotubes	No change	No change	-	1.5% (liquid state)/4.5% (solid state)	-	2019	[95]
Caprylic alcohol + Mynstyl alcohol (73.7:26.3 by mass)	0.3 wt% Multi walled carbon nanotubes	6.8 (decreased by 0.1)	168.2 (decreased by 0.5%)	0.2196	26.3%	Air conditioning	2015	[55]
Caprylic alcohol + Mynstyl alcohol (73.7:26.3 by mass)	0.4 wt% Al_3O_2	6.6 (decreased by 0.3)	167.9 (decreased by 0.7%)	0.1967	13.1%	Air conditioning	2015	[55]
Caprylic alcohol + Mynstyl alcohol (73.7:26.3 by mass)	0.8 wt% Fe_2O_3	6.5 (decreased by 0.4)	166.7 (decreased by 1.4%)	0.2297	32.1%	Air conditioning	2015	[55]

3.2. Microencapsulation of PCMs

Encapsulation of PCMs is a feasible technique to enhance heat transfer, which can prevent PCMs from mixing with the heat transfer fluid (HTF). Encapsulation is generally classified into macropackaging and microencapsulation according to their size. Microencapsulation refers to the use of a solid shell to encapsulate PCM particles with diameters from 1 to 1000 μm [96]. Macropackaging refers to loading the PCM into a macrocontainer made of metal or plastic with a capacity of several milliliters to several liters. Generally speaking, the capsules used for encapsulation have large specific surface areas and can adapt to thermal expansion/contraction during phase transition [97,98]. Heat exchange can be realized at approximately constant temperature, reducing the reactivity with surrounding materials. The same support materials can also be used to store or transport energy [99,100].

However, microencapsulation has the disadvantage of increasing the risk of supercooling. In addition, the low tightness of the shell material will cause the change of PCM composition if salt hydrate is used as the core material. Therefore, the current microencapsulation technology of PCMs is only applicable to organic PCMs. Table 7 lists some typical cases of microencapsulation to enhance PCM performance.

Xing et al. [101] prepared a kind of microencapsulated PCM for air conditioned cold storage by composite coacervation. Gelatin and gum acacia as encapsulating materials and tetradecane as core material were used to coat PCMs with low thermal conductivity into hydrophilic models of polymer capsules. Results showed that the initial melting temperature (Tm) was 5.792 °C, the latent heat at melting (ΔHm) was 191.919 J/g, the initial freezing temperature (Tf) was 2.375 °C, and the latent heat at freezing (ΔHf) was 189.173 J/g. The ΔHm of the material was consistent with the ΔHf, and the PCT also met the cold storage requirements of the air conditioner.

Xu et al. [102] prepared a microencapsulated PCM for air conditioning cold storage by a simple coacervation method, which used a mixture of tetradecane, pentadecane, hexadecane, or two or three of them as the core materials, and polymeric gelatin as the wall material. The PCT was 4–12 °C, suitable for an air conditioning inner cooler with a wide melting point range. Moreover, no leakage was observed before and after the phase transformation, protecting the refrigerator from clogging as well as prolonging its lifetime.

Dai et al. [103] used melamine–formaldehyde as wall material, n-tetradecane as core material, polyoxyethylene nonionic surfactant OP-10 as emulsifier, and styrene maleic anhydride as system modifier to prepare microcapsules by the in situ polymerization method. The DSC test showed that the Tm of the PCM was 5.6 °C, the crystallization temperature (Tc) was 5.2 °C, the ΔHm was 219.81 J/g, and the crystallization latent (ΔHc) heat was 220.58 J/g (pH = 3.5). The microcapsule PCMs were added to the holding layer inside the blood vessel box to test their performance at different external temperatures, and the experimental results showed that at the restrictive temperature of 45 °C, −25 °C, and room temperature of 23 °C, they could maintain the blood at 0–10 °C for 50.5, 80.7, and 61.7 h, respectively.

Yu et al. [104] synthesized a number of novel PCM microcapsules using n-octadecane/$CaCl_2$ as the core materials and calcium carbonate as the shell material by the self-assembly method. The Tc of the phase-change microcapsules was 23.54 °C, the Tm was 28.22 °C, the ΔHc was 65.32 J/g, and the ΔHm was 67.91 J/g when the mass ratio of n-octadecane/$CaCl_2$ was 40:60. The thermal conductivity was measured to be 1.325 W/(m·K), while that of the pristine solid-state n-octadecane was as low as 0.153 W/(m·K). It was found that the microencapsulated PCMs could consistently maintain stable PCT and enthalpy of phase transition, indicating their good thermal stability. This new PCM microcapsule is particularly suitable for making all-season protective clothing.

Wang et al. [105] synthesized phase change microcapsules by the self-assembly method with calcium carbonate as shell material and binary mixture of two paraffins, RT28 and RT42, as core materials. The PCT can be adjusted from 25 to 50 °C by adjusting the mass ratio of RT28 and RT42. FTIR showed that paraffin double core could be successfully encapsulated by the shell material. Microcapsules remained in shape after heating at 80 °C for 40 min without liquid leakage.

Table 7. Typical case of microencapsulation to enhance PCM performance.

Shell Material	Core Material	Method	Thermophysical Properties of Microcapsules	Key Findings	Applications	Year	Reference
Tetradecane	Gelatin gum Arabic	Complex coacervation	Tm 5.792 °C/Tf 2.375 °C; ΔHm 191.919 J/g/ΔHf 189.173 J/g	The ΔHm of the material is consistent with the ΔHf, and the PCT also meets the cold storage requirements of the air conditioner.	Air conditioner	2006	[101]
Polymer gelatin	Tetradecane, pentadecane, cetane	Simple coacervation	4–12 °C	It is not prone to leakage before and after phase transformation, protecting the refrigerator from clogging as well as prolonging the life of phase change cold storage agent.	Air conditioner	2004	[102]
Urea–Formaldehyde polymer	N-tetradecane (7.3 °C; 234 J/g)	In situ polymerization	7.1 °C; 147 J/g	The heat resistance of the coated microcapsules was significantly improved, and the weight loss rate decreased from 99.85% to 84.5%.	Thermal control system of spacecraft	2015	[103]
Melamine resin	N-octadecane (Tm 28.5 °C/Tc 25.0 °C; ΔHm 222 kJ/kg/ΔHc 222 kJ/kg) (64 wt%)	In situ polymerization	Tm 30 °C; ΔHm 141 kJ/kg/ΔHc 142 kJ/kg	The thermal stability of encapsulated n-octadecane was higher than that of pure octadecane, and the thermal decomposition temperature reached 160 °C.	Polyurethane foam board insulation	2010	[106]
Styrene (St) + Divinybenzen (DVB) copolymer (10:1)	Monomer + n-octadecane (1:1 by mass) (56.8 wt%)	Suspension polymerization	Tm 29 °C/Tc 16 °C; ΔHm 125 kJ/kg/ΔHc 127 kJ/kg	N-octadecane could be well coated in St-DVB copolymer to form a core/wall structure. The heat resistance of microcapsule material is about 230 °C.	Polyurethane foam board insulation	2010	[106]

Table 7. *Cont.*

Shell Material	Core Material	Method	Thermophysical Properties of Microcapsules	Key Findings	Applications	Year	Reference
Melamine-Formaldehyde resin	N-tetradecane (64.9 wt%)	In situ polymerization	Tm 5.6 °C/Tc 5.2 °C; ΔHm 219.81 kJ/kg/ΔHc 220.58 kJ/kg	At the limit temperature of 45, −25 and 23 °C, the blood can be maintained at 0–10 °C for 50.5, 80.7, and 61.7 h, respectively.	Blood insulation	2007	[103]
Polymethylmethacrylate (PMMA)	N-tetradecane	In situ polymerization	6.22 °C; 150.1 J/g	After 100 cold and heat cycles, the latent heat of microcapsules only decreased by 1.1 J/g, which has excellent thermal stability.	Temperature control packaging	2015	[107]
Polymethylmethacrylate (PMMA)	N-dodecanol + Decanol (50:50) (66.6%)	In situ polymerization	7.85 °C; 102.8 J/g	The coating rate of microcapsules is as high as 67.9%, and the maximum service temperature is not higher than 177.16 °C.	Temperature control packaging	2015	[107]
Calcium carbonate shell ($CaCO_3$)	N-octadecane + $CaCl_2$ (40:60 by mass) (43.53%)	Self-assembly method	Tm 28.22 °C/Tc 23.54 °C; ΔHm 67.91 kJ/kg/ΔHc 63.52 kJ/kg; thermal conductivity: 1.325 W/(m·K)	The thermal conductivity of solid original n-octadecane was 0.153 W/(m·K), and that of microcapsule was 1.325 W/(m·K). After 200 cycles of phase change, the PCT and enthalpy remained stable; the release rate of microcapsules after 30 days was 38.1%, indicating good impermeability.	All-season protective outfits	2014	[104]

Table 7. *Cont.*

Shell Material	Core Material	Method	Thermophysical Properties of Microcapsules	Key Findings	Applications	Year	Reference
Calcium carbonate shell ($CaCO_3$)	$CaCl_2$ + Paraffin RT28 (1:1 by mass)	Self-assembly process	Tm 20.93 °C/Tc 26.44 °C; ΔHm 57.7 kJ/kg/ΔHc 66.1 kJ/kg; thermal conductivity: 0.759 W/(m·K)	Compared with the original RT28 and RT42, the thermal conductivity is increased by 2–3 times. After heating at 80 °C for 40 min, the microcapsules had no liquid leakage.	Thermal management	2016	[105]
	$CaCl_2$ + Paraffin RT28 (1:2 by mass)		Tm 23.33 °C/Tc 27.41 °C; ΔHm 105.8 J/kg/ΔHc 107.2 kJ/kg; thermal conductivity: 0.714 W/(m·K)				
	$CaCl_2$/Paraffin RT28-RT42 (5:5) (1:1 by mass)		Tm 19.28 °C/Tc 27.44 °C; ΔHm 90.8 kJ/kg/ΔHc 95.9 kJ/kg; thermal conductivity: 0.739 W/(m·K)				
	$CaCl_2$/Paraffin RT28-RT42 (5:5) (1:2 by mass)		Tm 19.76 °C/Tc 27.67 °C; ΔHm 82.8 kJ/kg/ΔHc 122.8 kJ/kg; thermal conductivity: 0.701 W/(m·K)				
Polystyrene and Silica(PS-SiO_2)	N-tetradecane (Tet) (Tm 0.39 °C/Tc 2.15 °C; ΔHm 195.9 kJ/kg/ΔHc 194.2 kJ/kg)	In situ polymerization	Tm 2.13 °C/Tc 0.39 °C; ΔHm 83.38 kJ/kg/ΔHc 79.37 kJ/kg	The thermal conductivity of 5 wt% Tet + PS-SiO_2 slurry could reach 0.4035 W/(m·K) at 5 °C, and achieved an enhancement of 8.4% compared to Tet + PS slurry with same mass fraction.	Air conditioning systems	2016	[108]

Table 7. *Cont.*

Shell Material	Core Material	Method	Thermophysical Properties of Microcapsules	Key Findings	Applications	Year	Reference
Styrene-methylmethacrylate copolymer	N-octadecane	Miniemulsion in situ polymerization method	ΔHm 107.9 kJ/kg/ΔHc 104.9 kJ/kg)	After 360 thermal cycle tests, the Tc changed by 1.1 °C, the Tm changed by 0.6 °C, the ΔHm changed by 1.5 J/g, and the ΔHc heat changed by 1.2 J/g. No leakage was observed and the chemical stability was good.	Buildings	2014	[109]
Polyethylene glycol	SiO_2	Temperature-assistedsol–gel method	Tm 58.09 °C/Tc 42.34 °C; ΔHm 151.8 kJ/kg/ΔHc 141.0 kJ/kg)	The encapsulation rate is 79.3%, the encapsulation efficiency is 80.6%, and the thermal storage capability higher than 100%. The undercooling degree, melting time, and curing time of the composites were 22.3%, 26.5%, and 22.6% lower than those of the original polyethylene glycol, respectively.	Thermal energy storage applications in building envelopes	2015	[110]
Polystyrene	N-octadecane	Ultrasonic-assistant miniemul-sion in situ polymerization	124.4 kJ/kg	The nanocapsules were regular spherical and ranged from 100 to 123 nm in size. The PCT of nano encapsulated PCM was close to n-octadecane.	-	2008	[111]
Polystyrene	Nonadecane	Two-step Pickering emulsification procedure	Tm 34.12 °C/Tc 29.97 °C	The encapsulation rate is 55.9%. After 100 cycles, the PCT was almost unchanged and the thermal stability was good.	Thermal management	2015	[112]
Melamine formaldehyde	Dowtherm J	In situ polymerization	MEPCMS (LAES: 92.7–192.7 K, 207.9 kJ/kg/MEPCMS (PTES): 123–223 K, 123.6 kJ/kg	The shell curvature and solidification time of PCM microcapsules affect their heat transfer behavior and charging efficiency.	Cold storage	2018	[113]

3.3. Shape-Stabilized PCMs

The shape-stabilized PCMs (ss-PCM) are special PCMs composed of processing materials and support materials. PCMs are integrated with some solid porous matrixes, such as polymethacrylic acid, polyethylene, polystyrene resin, etc. Even if the working material changes phase, the supporting material remains in the solid state. The fabrication methods involve melting, physical blending (e.g., adsorbing, blending, impregnation), or chemical reaction (e.g., sol–gel method, graft copolymerization) [114–117]. Ss-PCMs can maintain a relatively shape-stabilized form during phase transition without containers. As a result, the ss-PCMs can be embedded in the building's envelope to reduce the cooling load [118]. Typical cases of shape-stabilized PCMs are listed in Table 8.

Zhang et al. [119] selected graphene oxide (GO) to shape polydiethylene glycol hexadecyl ether acrylate (PC16E2AC), and prepared ss-PCMs by the solution blending method. The morphological structure, thermal properties, and thermal stability of the composites were investigated. SEM photographs showed that pure PC16E2AC was relatively dispersed in the microscopic state; after the addition of GO, the GO surface sheets adsorbed PC16E2AC and made their compact composts together using the supporting effect of GO sheets. When the mass fraction of GO reached 5%, the PC16E2AC/GO composites began to precipitate at 105 °C, and the composites could maintain their initial shape at 85 °C for 100 min. The Tm and Tc of PC16E2AC/GO composites were 36.1 and 23.5 °C, respectively, and the latent heat was 71 J/g. The thermal performance was almost unchanged after 300 charging/discharging cycles.

Wu et al. [120] used polyurethane rigid foam (PU) to package octadecane, and used nanosilica as stabilizer and nucleating agent to prepare polyurethane ss-PCMs by the in situ encapsulation method. SEM images showed that the PCMs were homogeneously embedded among PU with good structural stability. FTIR curves also showed that no chemical reaction occurred between PU and PCM and no new functional groups were generated. When the mass fraction of PCM was 30%, the latent heat was 28 J/g, and the melting and solidification temperatures were 24.48 and 27.6 °C, respectively. Moreover, with the increase of mass fraction of PCM, the latent heat of ss-PCMs increased gradually, but the PCT remained stable, indicating the good compatibility between PU and PCM.

Ma et al. [121] used porous graphite as matrix and capric acid lauric acid (CA–LA) eutectic as PCMs to prepare capric acid–lauric acid/expanded graphite (CA–LA/EG) by physical adsorption. The ESEM diagram showed that CA–LA was effectively encapsulated in porous graphite, and the expanded graphitic pore structure still maintained the network structure. DSC graphs showed that the PCT and latent heat of CA–LA were 19.63 °C and 115.80 J/g, respectively, and those of CA–LA/EG were 19.50 °C and 93.18 J/g, respectively. The mass ratio of CA–LA in CA–LA/EG was approximately equal to the enthalpy ratio, i.e., 80.47%.

Yang et al. [64] prepared a binary PCM composed of 82% lauryl alcohol (LA) and 18% stearic acid (SA) with a Tm of 21.3 °C and a latent heat of 205.9 kJ/kg. The composite ss-PCM was prepared by the vacuum adsorption method using expanded perlite and ceramsite as porous adsorption materials. It was observed by SEM that the PCM was saturated in ceramsite, and the pores on the surface of expanded perlite were basically filled with PCM. FTIR results showed that there were no new characteristic peaks in the preparation of the composite setting materials, LS–SA/expanded perlite and LA–SA/ceramsite, indicating that there was no chemical reaction in the adsorption process. The TG results showed that the mass decline rates of LS–SA/expanded perlite and LS–SA/ceramsite samples were 1.5% and 1.1%, respectively, in the temperature range of 0–120 °C. DSC analysis curves indicated that expanded perlite had less influence on the thermal properties after encapsulation; the Tm and latent heat of LS–SA/expanded perlite were 22.7 °C and 165.3 kJ/kg, while those of LS–SA/ceramsite were 22.5 °C and 133.4 kJ/kg.

Table 8. Typical cases of shape-stabilized PCMs.

PCM	Support Materials	Method	Thermophysical Properties of ssPCM	Key Findings	Applications	The Published Year	Reference
Poly (diethylene glycol hexadecyl ether acrylate) (PC16E2AC)	Graphene oxide (GO)	Solution blend	Tm 36.1 °C/Tc 23.5 °C; ΔHm 71kJ/kg/ΔHc 71 kJ/kg	When the mass fraction of GO is 5%, PC16E2AC starts to precipitate at 105 °C, and the PC16E2AC/GO composite maintains its initial shape at 85 °C for 100 min. After 300 cold and hot cycles, the PCT and latent heat remain unchanged, and has good thermal resistance cycle.	-	2016	[119]
Oetadecane (30 wt%)	Rigid polyurethan (PU)	In situ preparation	Tm 24.48 °C/Tf 27.60 °C; ΔHm 28.93 kJ/kg/ΔHf 27.96 kJ/kg	The prepared polyurethane ss-PCM had a micro nano uniform microstructure, the PCMs were evenly distributed in the polyurethane, and PU had good compatibility with PCM.	Building materials	2012	[120]
Capric acid + Lauric acid (61.13:38.87 by mass) (19.63 °C; 115.80 J/g)	Porous graphite	Physical adsorption	19.50°C; 93.18 J/g	The low temperature eutectic PCMs accounted for 80.47% of the fixed PCMs. Compared with the original PCMs, the melting time and solidification time of the composite materials decreased by 74.1% and 84.9% respectively. There was no liquid exudates during the phase change process.	-	2010	[121]

Table 8. *Cont.*

PCM	Support Materials	Method	Thermophysical Properties of ssPCM	Key Findings	Applications	The Published Year	Reference
Lauryl alcohol (LA) + Stearic acid (SA) (82:18 by mass) (21.3 °C; 205.9 kJ/kg)	Expanded perlite	Vacuum adsorption	22.7 °C; 165.3 kJ/kg	The adsorption performance of expanded perlite on PCMs was significantly higher than that of ceramsite. After vacuum adsorption for 3 h, the adsorption rate of LA–SA was up to 352.5%, which was about 7.4 times that of ceramsite with equal mass. LA–SA combined well with the two porous materials, and the adsorption process was only physical adsorption, meanwhile, LA–SA did not volatilize in the range of 0–120 °C. Compared with ceramsite, expanded perlite had less effect on the thermal properties of LA–SA after encapsulation.	Building materials	2020	[64]
	Ceramsite		22.5 °C; 133.4 kJ/kg				
Borax + $Na_2SO_4 \cdot 10H_2O$ (2% + 90%)	Expanded graphite (8%)	Vacuum adsorption	225.77 kJ/kg; undercooling 0.6 °C	There was no liquid exudation after phase transformation. Compared with $Na_2SO_4 \cdot 10H_2O$ only adding borax, the heat storage time was shortened by 52.6%, the heat release time is shortened by 55.1%, and there was no performance attenuation after 500 heat storage/release cycles.	-	2015	[122]
$CH_3COONa \cdot 3H_2O$ + $Na_2HPO_4 \cdot 12H_2O$ (91% + 1%)	Expanded graphite (6%)		233.5 kJ/kg; no undercooling; no phase separation	There was no liquid exudation after phase transformation. Compared with only adding KH_2PO_4, the heat storage time was shortened by 75.3%.			
$Ba(HO)_2 \cdot 8H_2O$ + KH_2PO_4 (93% + 1%)	Expanded graphite (6%)		248.3 kJ/kg; undercooling less than 0.5 °C	There was no liquid exudation after phase transformation, and the heat storage time was shortened by 45.1% and the heat release time was shortened by 54.5% compared with the pure material.			

Table 8. *Cont.*

PCM	Support Materials	Method	Thermophysical Properties of ssPCM	Key Findings	Applications	The Published Year	Reference
Lauric acid	Expanded perlite	Vacuum adsorption	45 °C	Expanded perlite had a good adsorption capacity for lauric acid. lauric acid did not exudate when the content of lauric acid was less than 30%.	-	2014	[123]
Buytle stearate (20 °C; 140 J/g)	Plaster board	Physical adsorption method	20.08 °C; 51.8418 J/g	Under the negative pressure state, the adsorption temperature of 25 °C for 5 min, the retention rate reached 60%, the thermal conductivity of gypsum board was 7% higher than that of pure gypsum board, and the retention rate decreased by 0.8% after 30 freeze–thaw cycles.	Buildings	2010	[124]
	Expanded perlite		20.40 °C; 92.2015 J/g	The retention rate of PCM was 180%, and the loss rate was 0.7% after 30 freeze–thaw cycles.			
Polyethylene glycol	Active carbon	Physical blending and impregnating method	-	It had good heat resistance below 250 °C.	-	2011	[125]
Paraffin wax (70 wt%) + liquid paraffin (30 wt%) (29.94 °C; 145.9 J/g)	Calcined opal	Fusion adsorption method	Tm 24.91 °C/Tf 24.87 °C; ΔHm 59.04 kJ/kg/ΔHf 56.26 kJ/kg	In the molten state, there was no leakage of liquid paraffin in the composite, and there was no obvious change in the PCT and latent heat after 200 thermal cycles.	Indoor energy storage building materials	2013	[126]
Capric acid	Expanded perlite	Vacuum impregnation method	Tm 31.8 °C/Tf 31.6 °C; ΔHm 98.12 kJ/kg/ΔHf 90.06 kJ/kg	After 5000 thermal cycles, Tf decreased by 0.09 °C, Tm decreased by 1.55 °C, ΔHm decreased by 2.6%, and ΔHf increased by 0.6%, indicating good thermal reliability and chemical stability.	Buildings	2008	[127]

Table 8. *Cont.*

PCM	Support Materials	Method	Thermophysical Properties of ssPCM	Key Findings	Applications	The Published Year	Reference
Liquid paraffin + Octadecane (4:6 by mass) (16.9 °C; 124.2 J/g)	High density polyethylene (HDPE)	Melt blending method.	72.22 J/g	With the increase of the carrier content, the latent heat of the composite PCMs synthesized using HDPE as the carrier decreased slowly, which had little effect on PCT, and the optimal carrier proportion was 30%.	-	2020	[128]
Dodecane	Expanded graphite (EG)	Vacuum infiltration method	−9.67 °C; 151.7 J/g	Dodecane was evenly embedded in the pores of EG with a thermal conductivity of 2.2745 W/(m·K); EG can reduce the liquid leakage of dodecane.	Cold chain logistics	2019	[129]

3.4. A Complex of Organic and Inorganic Salt Solutions

Yang et al. [130] developed a composite low-temperature PCM applied to storage freezers (−20 to 0 °C) by mixing and stirring ammonium chloride solution with ethylene glycol. DSC measurements showed that the initial melting temperature of 25% ethylene glycol solution was −11 °C, the peak melting temperature was −18 °C, and the melting latent heat was 96.8 kJ/kg. For 15% ammonium chloride solution, these values were −13 °C, −16 °C and 336.6 kJ/kg, respectively. When 25% ethylene glycol solution and 15% ammonium chloride solution were mixed in the ratio of 2:3, the PCT of the mixed solution was −16 °C, and the latent heat was 212.8 kJ/kg, significantly greater than that of ethylene glycol solution; meanwhile, no supercooling phenomenon was observed substantially. However, due to the large temperature difference between the cryogenic refrigerator and the PCMs, a certain temperature fluctuation occurred in the early stage of solidification of the hybrid materials.

Huang et al. [131] developed a composite cold storage material for application in cold chain stream using aqueous sodium formate (26 wt% $CHNaO_2$) as the base fluid material with the addition of KNO_3. It was found that the composite cold storage material with the addition of 11% KNO_3 exhibited good thermal properties: PCT of −18.002 °C, phase transition latent heat of 279.1 kJ/kg, and thermal conductivity of 1.182 W/(m·K). Compared with 26% aqueous $CHNaO_2$ solution, the latent heat value increased by 9.8% and thermal conductivity increased by 16.4%. The PCT met the transportation storage demands of the most economical storage temperature of –18 °C for most frozen products.

Wang et al. [132] mixed aqueous CH_3CH_2OH (15 wt%) and aqueous NH_4Cl (25 wt%) solutions at a certain mass ratio and added a superabsorbent polymer (SAP) to prevent liquid leakage of PCMs. The viscous outdoor PCM realized was measured to have a PCT of −17.1 °C and a latent heat of 304 J/g. The use of PCM could effectively enhance the rapid freezing of food; for example, the central temperature of 25 mm thick chicken meat decreased from−1 to −5 °C in 55.5 min.

Typical cases of composite organic and inorganic salt solutions for PCMs are listed in Table 9.

Table 9. A complex of organic and inorganic salt solutions for PCM.

Organic PCMs	Inorganic PCM	Composite PCT (°C)	Composite Latent Heat (kJ/kg)	Thermal Conductivity of Composites (W/(m·K))	Application	Reference
25% Ethylene glycol solution (−11 °C; 96.8 kJ/kg)	15% NH_4Cl solution	−16	212.8	-	Refrigerator	[130]
26 wt% Sodium formate aqueous solution (−14.8 °C; 254.2 kJ/kg; 1.015 W/(m·K))	11 wt% KNO_3	−18	279.1	1.182	Cold chain logistics	[131]
15 wt% CH_3CH_2OH aqueous solution	25 wt% NH_4Cl aqueous solution	−17.1	304	-	Freezer compartment of refrigerator	[132]
$C_6H_7KO_2$ (5 wt%)	KCl (25 wt%)	−14	230.5	-	Preservation of frozen food	[133]
$C_6H_7KO_2$ (25 wt%)	KCl (5 wt%)	−18.6	131.91	-		
$C_{10}H_{14}N_2Na_2O{\cdot}2H_2O$ (15 wt%)	KCl (15 wt%)	−16.7	-	-		
HCO_2Na (5 wt%)	KCl (25 wt%)	−23.6	261.2			
HCO_2Na (10 wt%)	KCl (20 wt%)	−23.8	266.4			
HCO_2Na (15 wt%)	KCl (15 wt%)	−23.8	263.3			
HCO_2Na (20 wt%)	KCl (10 wt%)	−23.5	254.8			
HCO_2Na (22 wt%)	KCl (8 wt%)	−23.8	250.3			
HCO_2Na (25 wt%)	KCl (5 wt%)	−23.8	263.3			

4. Applications of PCMs for CTES

4.1. Buildings

The applications of CTES systems based on PCM in the buildings can be categorized into two types: passive and active systems. In passive systems, PCM is integrated into building materials such as wallboard, glass, roof, solar chimney, and floor. When the indoor or outdoor temperature rises or falls beyond the Tm of PCMs, the stored heat or cooling capacity will be automatically released [134]. Passive systems have low initial investment and operation cost, but small energy storage capacity. In active systems, the CTES is combined with the traditional HVAC system as an integral part. Its main advantages are reducing the size of equipment, lowering the capital and operation costs, saving energy, shifting peak power, and improving system operation [135–137]. Table 10 lists some of the latest applications of PCM cold storage in buildings.

Maccarini et al. [138] developed a PCM-based heat exchanger model, which stored cold at night and released cold through water circuits during the day. PureTemp 18, a material with a melting point of 18 °C was selected considering that ambient air temperature was 16 °C during the summer night in Copenhagen, Denmark. A year-round simulation of a typical model of an office building showed that integrating a free cooling unit could significantly reduce the primary energy utilization of the new HVAC system. The use of mechanical cooling could almost be completely avoided, resulting in a yearly energy saving of approximately 67% compared to the baseline plant configuration.

Piselli et al. [139] used the numerical analysis method to optimize the performance of integrated PCMs in building envelopes. The PCM plates used were gypsum plates containing 30 wt% microencapsulated paraffin, integrated into the innermost layer in the stratigraphy of the roof and the external walls. The simulation results showed that the cooling saving could reach 300 kWh/year under mild climate. Simultaneously coupling PCMs with temperature controlled natural ventilation strategies could reduce the cooling demand by more than 65% in moderate climate zones.

Piselli et al. [140] also developed a novel organic eutectic PCM with high storage capacity for CTES. The eutectic PCM includes lauryl alcohol and stearyl alcohol (90:10). The Tm and latent heat of the new eutectic PCM were 22.93 °C and 205.79 J/g, respectively. The thermal conductivity of the PCM was 0.18 W/(m·K). The discharge experiment showed that the cold energy stored in the PCM could keep the room temperature at 3.5 °C lower than the ambient temperature for 6.78 h, which can greatly save electric energy.

Rucevskis et al. [141] designed a PCM-based active TES system for cooling multistory residential buildings. The TES system is integrated under the concrete ceiling inside the building to cool the PCMs (paraffin RT22HC) at night through cold water flowing in a capillary system contained in the energy storage unit. The latent heat of the PCM is 160 kJ/kg and the PCT is 20–23 °C. Numerical results showed that the active TES system could reduce the indoor temperature by 9.5 °C.

Table 10. Typical applications of PCMs for CTES in buildings.

PCM	Phase Change Temperature of PCMs	Building Characteristics	Research Method	Application Form	Key Findings	Year	Reference
PureTemp 18	18 °C	A three-story office building model	Numerical	HVAC system	The integration of free refrigeration units can significantly reduce the primary energy utilization of HVAC systems. Compared with the baseline thermal plant configuration, the annual energy primary energy saving was about 67%.	2018	[138]
Microencapsulated paraffin	23–26 °C	Four story rectangular apartment building model (in Italy)	Experimental	A PCM board was integrated in the roof and the external walls of the building.	In milder climates, the cooling demand was reduced by more than 65%.	2020	[139]
Lauryl alcohol + alcohol (90:10)	22.93 °C	A 1.7 m × 1.7 m × 2.6 m air conditioned test room	Experimental	Air conditioning system	The 10 kg eutectic PCM released the stored cold air for 6.78 h until the end of the discharge cycle, and the bottom chamber temperature was about 3.5 °C lower than that without PCM.	2020	[140]
Paraffin RT22HC	20–23 °C	A living room with dimensions of 6 m × 6 m × 3 m in a typical second floor apartment of a multistory residential house	Numerical	Integrated under the concrete ceiling slab of the building interior	Reduce the indoor air temperature by about 9.5 °C.	2020	[141]
Liquid paraffin	Tm 25.22 °C/Tf 28.88 °C	Two identical test rooms of 1.7 m × 1.7 m × 2.1 m (in Tianjin)	Experimental	Composite PCM wallboard	The PCM room had less temperature fluctuation, lower peak temperature, and smaller lag time than the reference room.	2017	[142]

Table 10. *Cont.*

PCM	Phase Change Temperature of PCMs	Building Characteristics	Research Method	Application Form	Key Findings	Year	Reference
Commercial macroencapsulated PCM-RT25HC	25 °C	Two identical experimental huts of 2.4 m × 2.4 m × 2.4 m (at the University of Auckland, New Zealand)	Experimental	Combination with an air-based solar collector	PCMs store free cooling capacity during the summer night, reducing indoor temperature fluctuation and cooling load.	2020	[143]
Organic alcohol PCMs	33.1–35.1 °C/41.7–42.7 °C	Two identical test rooms (at Tongji University in Shanghai)	Experimental	Novel diatomite-based composite PCM wallboards (PCMW)	PCMW was attached to the external wall surface of the test room, and the external surface temperature of PCMW was lower than that of traditional polystyrene plastic insulation wallboard.	2020	[144]
-	22–24 °C	A south-facing middle office room located in Beijing	Numerical	Ventilation system	When the indoor temperature set point was 24–28 °C, the energy saving of the system using PCM energy storage was 16.9–50.8%, while that of traditional night ventilation system was 9.2–33.6%.	2019	[145]
Octadecane	Tm 23.33 °C/Tc 20.58 °C	Two small test rooms of 1.22 m × 1.22 m × 1.22 m (in Tabriz, Iran)	Experimental	Nanoencapsulated PCM/plaster wallboard	The PCM system reduced indoor air temperature fluctuations and maintained the thermal comfort throughout most of the year.	2020	[146]
DuPont Energain PCM panels	18–24 °C	A test chamber 2.80 m wide × 1.30 m deep × 2.44 m high located in a large climate chamber with dimensions of 8.9 m × 7.3 m × 4.7 m	Experimental	Embedded on the back wall of a test hut placed in the climatic chamber	After the end of February in Montreal, energy consumption decreased by 20%.	2015	[147]
Commercial organic materials (RT11HC)	10–12 °C	Cold storage (in Fuzhou, China)	Numerical	Coupled with cold storage heat pump system	While under the demand tariff, the electricity charge saving ratio of the cold storage system over the conventional system was 9.07–11.28%	2020	[148]

4.2. Refrigeration

The traditional refrigeration technology is mainly based on the mechanical compression refrigeration with low energy efficiency. Using the PCMs-based CTES can reduce the switching frequency of a refrigeration device for energy saving. Table 11 lists the typical recent applications of cold storage PCMs in refrigeration.

Ezan et al. [149] investigated the effect of a PCM slab integrated inside a vertical beverage cooler (VBC) on energy consumption, thermal stability, and air flow characteristics inside the chillers. Considering the average evaporation temperature of VBC (Tevap, av≈ -10 °C) and the working limit of the thermostatic controller, water was chosen as the PCM. The PCM slab was placed on the back of the flat plate roll evaporator with different thicknesses (2, 4, 6, 8, and 10 mm), in direct contact with the air. The three-dimensional and transient models of forced convection were established. The CFD simulation by ANSYS-FLUENT showed that the implementation of PCM slab prolonged the duration of the first descent, compressor closing and opening. The frequency of the compressor switching cycle with 2 mm PCM slab was reduced by nearly 10 times. When the thickness increased to 6 mm, the compressor operating time ratio decreased from 36% to 26%.

Du et al. [150] numerically studied a portable cold box for cold chain application based on PCMs. PCMs used in the study were RTO, RT2HC, RT3HC, RT4HC, RT5HC, and RT8HC from Rubitherm Company (Berlin, Germany). The results showed that the configuration position of the PCM module could significantly affect the cooling time. The melting point of the PCM also affected the cooling time, but the effect was smaller compared to the location. The insulation materials with a lower thermal conductivity might cause a longer cooling time. The configuration of PCM (melting point at 2 °C) with 20% located on the top and 20% on each of the side walls coupled with the vacuum insulated panel (VIP) could result in the longest duration time. The maximum cooling time could reach 46.5 h with the maximum discharging efficiency at 90.7% and the highest discharging depth at 99.4%, offering a great potential for cold chain applications. Meanwhile, the price of VIP insulating boxes of the same size was 2.5 times higher than that of PU.

Zhao et al. [50] used lauryl alcohol and tetradecane as the main refrigeration materials and expanded graphite as additives to develop an efficient and low-temperature PCM for pharmaceutical cold chain logistics (2–8 °C). The PCT of the material was 4.3 °C, the latent heat was 247.1 J/g, and the thermal conductivity was 0.9657 W/(m·K). In order to ensure more uniform release and transfer of cold heat from cold storage facilities, a novel vaccine cold storage cassette was developed. The low-temperature PCMs developed in combination with refrigerated equipment loading experiments were conducted on yoghurt as the object (the storage temperature of yogurt in shipping refrigerators is 2–8 °C). It was found that the average holding time was 46.04 h and the yogurt effective holding time was 50.02 h. The new cold chain transport equipment developed could guarantee the required low temperature environment of a vaccine for a long time during transport.

Zarajabad and Ahmadi [151] studied a CTES system using PCM in household refrigerator with ceiling evaporator. Fins were added to the PCM container to enhance heat transfer. The experimental results showed that the compressor equipped with CTES system worked for 3.566 h per day, and the working time was reduced by 45 min compared with that without the CTES system. The energy consumption of the compressor was reduced by 17.4% per day, and the fossil fuel consumption and carbon dioxide emission of 12 L and 28 kg could be reduced, respectively.

Table 11. Typical applications of cold storage PCMs in refrigeration.

Applications	Characteristics of the Application	PCM	PCT of PCM	Research Method	Key Findings	Year	Reference
Vertical beverage cooler (VBC)	A commercial VBC with a storage capacity of 360 L, 1.65 m high, 0.65 m wide, and 0.55 m deep, with an average evaporation temperature of −10 °C	Water	0 °C	Numerical	The first pressure drop, compressor start and close time were prolonged. A 6 mm thick PCM board reduceed the compressor running time ratio from 36% to 26%.	2017	[149]
Portable cold box for cold chain	The outer dimensions of the portable box are 430 mm in length, 285 mm in width and 345 mm in height; the internal dimensions are 355 mm in length, 215 mm in width and 265 mm in height	RTO, RT2HC, RT3HC, RT4HC, RT5HC, RT8HC	0, 2, 3, 4, 5, 8 °C	Numerical	The melting point was 2 °C, the PCM arrangement was 20% at the top and 20% at each side wall, and the VIP was employed inside the box; this configuration had the longest cooling time of 46.5 h, the largest discharge efficiency of 90.7%, and a discharge depth of 99.4%.	2020	[150]
Refrigerated box for transporting a vaccine	Refrigerator box with effective volume of 2 L and internal size of 285 mm × 285 mm × 285 mm. The refrigeration board is made of polyethylene, and the thermal insulation material is vacuum thermal insulation board (vaccine transportation and storage temperature: 2–8 °C)	Tetradecane + lauryl alcohol + expanded graphite	4.3 °C	Experimental	Combined with refrigeration equipment, the low temperature PCM developed could maintain the vaccine box at 2–8 °C for the longest time of 52.36 h.	2020	[50]
Household refrigerator	A 16-foot high household refrigerator with a size of 50 cm^3 × 60 cm^3 × 155 cm^3 and a wall thickness of 3.7 cm (temperature range: 1–5 °C)	Water	0 °C	Numerical + experimental	The PCM equipment equipped with three fins could maintain the temperature in the refrigerator compartment within the standard range for 68 min and reduce the working time of the compressor for 45 min.	2018	[151]

Table 11. *Cont.*

Applications	Characteristics of the Application	PCM	PCT of PCM	Research Method	Key Findings	Year	Reference
Refrigerated panels for small distributed refrigerated transport facilities	The refrigeration panel is made of plexiglass, with internal dimensions of 180 mm long, 80 mm wide and 160 mm high; six HPs are integrated into the panel and immersed into the PCM	Water	0 °C	Experimental	A low temperature energy storage panel with HPs embedded in PCM was developed. The effects of air speed and air temperature on the discharge performance of PCM were analyzed. The air side temperature difference increased with the increase of inlet air temperature and decreased with the increase of wind speed.	2020	[152]
Open display cabinet in supermarket	The display cabinet is 1.3 m long, 0.9 m wide and 2.0 m high; there is no door on the display cabinet (cool food storage temperature: 0–6 °C)	Water	0 °C	Experimental	PCM was introduced into the finned tube heat exchanger at the air duct behind the display case. After the compressor was shut down for 2 h, the temperature rise of the product was only 1 °C when the ambient temperature was 16 °C.	2019	[153]
Multitemperature zone cold storage incubator for cold chain logistics	Equipment 1: large cold storage equipment with storage capacity of 680 L, internal size of 1450 mm × 750 mm × 650 mm and three temperature zones is used for fruit and vegetable products with large transportation volume; equipment 2: the storage volume is 16 L, the internal size is 30 mm × 30 mm × 30 mm, and a small cold storage refrigerator with two temperature zones is set for the transportation of medical vaccines	PCM1: 87% $C_8H_{16}O_2$ + 13% $C_{14}H_{28}O_2$/PCM2: H_2O + 0.03 g/mL $C_6H_2KO_2$	PCM1: 7.1 °C/PCM2: −2.5 °C	Experimental	A large and a small multitemperature zone cold storage incubator were designed by coupling two kinds of PCMs with vacuum insulation plate technology. The temperature of medium temperature zone 2 of the large incubator was between 7 °C and 9 °C for about 13 h. The temperature of the phase transition process in temperature zone 3 was maintained at about −2–0 °C for 14 h. The temperature of medium temperature region 1 of equipment 2 was 7–8 °C for about 19 h. The PCT in temperature zone 2 was 0 °C, and the temperature was kept cold for about 16 h.	2019	[154]
Cold plate of refrigerated container in truck	A 6-ton truck with refrigerated container, with container size of 2.05 m × 2.2 m × 4.8 m	Sub zero eutectic PCM solution: E-26, E-29, E-32	E-26: −26 °C, E-29: −29 °C, E-32: −32 °C	Experimental	When the speed of the truck was 110 km/h, the maximum driving distance of the truck was 491 km when loaded with PCM E-26.	2020	[155]

Table 11. *Cont.*

Applications	Characteristics of the Application	PCM	PCT of PCM	Research Method	Key Findings	Year	Reference
Combined with solar energy for refrigerator cooling and energy	A hybrid solar power refrigeration system using low temperature thermal energy storage	Diethylene glycol	−10 °C	Numerical	Total irreversibility and total energy efficiencies were 908.2 kW and 45.14%, respectively.	2020	[156]
Refrigerator freezer	The cold accumulator is placed in the freezer of the refrigerator to exchange heat with the evaporator	CH_3CH_2OH aqueous solution (15 wt%) + NH_4Cl aqueous solution (25 wt%)	−17.1 °C	Experimental	The central temperature of chicken was lowered from −1 to −5 °C in 55.5 min.	2015	[131]
New chilly bins for food storage.	Chilly bin with inner diameter of 110 mm, length of 270 mm and polystyrene insulation	PT-15	−15 °C	Numerical + experimental	When PCMs were used in chilly bin, the maximum time to ensure a good food storage temperature could reach 240 min, and the transportation/storage time could be increased by 400%.	2013	[157]
PCM package for commercial ice cream containers	Widely commercial 5 L ice cream containers contain 2 cm PCM at the bottom	E-21	−21.3 °C	Numerical + experimental	After placing the ice cream outside the refrigerator for 3 h, the average temperature of the ice cream was –15 °C, which was 3 °C lower in the center of the container and 10 °C lower in the corner of the container than that without PCM.	2013	[158]
Thermal protection for ice cream storage/transportation	220 mm × 150 mm × 25 mm PCM rectangular brick	An eutectic solution of water and sodium	−21 °C	Experimental	When containers were exposed to ambient temperatures for 40 min, the temperature change in all areas of ice cream was limited to less than 1 °C.	2015	[159]
Refrigeration system of refrigerated truck	The PCM is encapsulated in a 1.7 m × 0.2 m × 0.02 m flat container, and 19 parallel PCM boards are contained in a well-insulated shell	An inorganic salt-water solution	−26.7 °C	Experimental	When the initial temperature of the cooling chamber was −7 °C and the ambient temperature was 30 °C, the cooling chamber gradually cooled to −15.8 °C after about 2 h.	2012	[160]
Mobile refrigeration system	The PCM is encapsulated in a flat plate of 1.6 m × 0.52 m × 0.02 m	An inorganic salt-water solution	−26.7 °C	Simulation	In Adelaide climate, the temperature of the refrigeration room could be maintained at −18 °C for 10 h.	2014	[161]

Table 11. *Cont.*

Applications	Characteristics of the Application	PCM	PCT of PCM	Research Method	Key Findings	Year	Reference
Refrigerated open display cabinet	A PCM container acts as an auxiliary evaporator during compressor shutdown	Hydro gel PCM composed of deionized water, silver iodide, guar and sodium tetraborate	−2 °C	Simulation	Compared with the basic cabinet, the defrosting and compressor shutdown intervals of the cabinet with PCM were extended by 98% and 50%, respectively, and the startup and shutdown of compressor was reduced by 27%.	2016	[162]
Display cabinet for food refrigeration	A new shelf with HPs and PCMs	98% deionized water + 2% borax	−0.5 °C	Experimental	The combination of HP and PCM reduced the temperature rise of food during thawing by 1.5 °C and improved the temperature uniformity of food.	2010	[163]
Refrigerated display container	Two single plate radiators act as PCM heat exchangers	Deionized water + 1.2% silver iodide + 0.9% guar + 0.15% sodium tetraborate	−2 °C	Experimental	The cabinet with PCM could save energy by about 5%, and the defrosting time was about 5 min longer than the basic cabinet.	2015	[164]
Plate freezing of fish on small fishing boats	Shell and tube heat exchanger with PCM	CO_2	−57 °C	Numerical + experimental	The freezing time was reduced by more than 3%, and the fish yield increased by 2.9%.	2019	[165]
Large poultry processing plant	Integrated in industrial NH_3/CO_2 Cascade Refrigeration System	AdBlue	−11 °C	Simulation	Compressor power decreased by 19% during discharge.	2018	[166]
Fish industry tunnel freezer	NH_3/CO_2 Cascade	CO_2	<−50 °C	Numerical	The required power could be reduced by up to 30% at the same refrigeration capacity.	2011	[167]
Refrigerated truck	Eight PCM cold plates with size of 80 mm × 40 mm × 4 mm	Eutectic salt	−21.2 °C	Simulation	Vehicle interior temperature could be maintained for 73.6 h at 293 K ambient temperature.	2017	[168]
Refrigerated transport	Nineteen parallel PCM plates with the size of 0.26 m × 1.70 m × 0.025 m are located in the refrigerator with the size of 3.4 m × 2.2 m × 2.2 m	-	Tm −26.7 °C/Tf −30.6 °C	Numerical + experimental	The established one-dimensional liquid-based mathematical model for flat-plate phase change heat storage unit agreed well with the experimental verification results.	2011	[169]

Table 11. *Cont.*

Applications	Characteristics of the Application	PCM	PCT of PCM	Research Method	Key Findings	Year	Reference
The cold chain for the Ebola vaccine	Aluminium PCM block	PlusICE E-78	−78 °C	Experimental	The Deep Freeze Arktek, when combined with PCM, maintained temperatures <−60 °C for 6.5 days in 43 °C ambient with a heat leak of 2.2 W.	2015	[170]
Household refrigerator	Double energy storage refrigerator (DES) with heat storage condenser (HSC) and cold storage evaporator (CSE)	Undecane (located in evaporator)/paraffin (located in condenser)	−26 °C/50 °C	Numerical	DES had higher evaporation pressure and temperature, and the energy saving was up to 32%.	2017	[171]
Storage and transportation of low temperature frozen food	The PCM is encapsulated in a thin stainless steel container and placed on the tube of the evaporator, accounting for 3.36% of the internal volume of the storage unit	ClimSel C-18/Cristopia E-21	−18 °C/−21.3 °C	Experimental	Using E-21 as PCM could maintain lower (−16/−12 °C) air temperature and longer time than C-18 (−12/−7 °C).	2012	[172]
Freezer	The PCM is encapsulated in an aluminum plate and placed on the refrigerator wall	An eutectic composition of water and ammonium chloride	−15.4 °C	Experimental	Compared with the refrigerator without PCM, the refrigerator with PCM panel had lower temperature fluctuation, smaller ice cream crystal size, and less drip loss of frozen meat.	2010	[173]
Household refrigerator	PCM encapsulated in cubic copper container with size of 2 cm × 28 cm × 43.5 cm	NaCl-H_2O	−21.15 °C	Numerical	The PCM–CTES could keep the refrigerator under standard thermal conditions for 4.5 h.	2017	[174]
Small low-cost space mission	Cooling a spaceborne atmosphere	Methanol	−97 °C	Experimental	If the heat load entering the system is low enough to maintain the PCMs close to equilibrium, the constant temperature can be maintained during freezing and melting.	1995	[175]

4.3. Thermal Management of Electronic Equipments

Under a high discharge rate, part of the energy released inside a lithium-ion battery makes the operating temperature of the battery higher than its acceptable range (60 °C) [176], which will reduce the battery power performance and lifetime. Overheating of chips in electronic equipment may also lead to system failure. This heat dissipation needs to be removed by an effective cooling system. The PCM-based thermal management cooling system will store the heat of electronic equipment during the high power period, so as to keep the temperature of electronic equipment within the allowable range and evenly distributed, ensuring the safety and extended service life of the equipment. Table 12 lists typical applications of PCMs in thermal management of electronic equipment.

Heyhat et al. [177] examined the thermal performance of passive thermal management systems using PCMs. The effects of using nanomaterials, fins, and porous metal foam beside PCMs were compared. The results indicated that porous-PCMs had higher performance than nano-PCMs and fin-PCMs. The use of porous-PCMs resulted in a 4–6 K decrease in the average temperature of the lithium-ion batteries compared with pure PCMs. Nevertheless, in the case of porous-PCMs, a time delay was observed during the melting onset process, which could degrade the performance of the battery thermal management system.

Table 12. Typical applications of cold storage PCMs in thermal management of electronic equipment.

PCM	Properties of PCM	Application	The Characteristics of Electronic Devices	Working Conditions	Research Method	Key Findings	Year	Reference
N-eicosan	309.55–309.65 K	Thermal management of lithium-ion batteries	The 18,650 lithium-ion battery is located on the central axis of the aluminum housing. The inner diameter of the shell is 31 mm, the wall thickness is 5 mm and the height is 70 mm. The diameter of the battery is 18 mm and the height is 65 mm.	High yield heat rate (4.6 W and 9.2 W)	Numerical	Using the porous-PCM led to 4–6 K reduction in the battery mean temperature.	2020	[177]
Carbon fiber–paraffin composites	42–49 °C	Thermal management of a Li-ion battery	A regular AA Li-ion battery (e.g., 14500AA)	The heat production rate is 2 W.	Experimental	PCM + 2-mm-long carbon fibers (0.46%) showed the best thermal performance; a 45% reduction of maximum temperature rise of the battery simulator could be achieved.	2015	[178]
Paraffin/aluminum foam composite PCM	46–52 °C	Battery modules in electric vehicles	The commercial rectangular $LiFePO_4$ battery (119 mm in length, 70 mm in width, and 27 mm in height)	Lithium-ion batteries are charged at 1 and 2 °C rates.	Experimental	The addition of composite PCM reduced the maximum surface temperature rise of lithium-ion batteries by 53%.	2015	[176]
Paraffin wax	56–58 °C	Electronic thermal management of round pin-finned heat sink	Round pin-fin heat sinks	Input power densities of 1.6 to 3.2 kW/m^2 witha step of 0.4 kW/m^2	Experimental	Heat sink with PCM volume fraction of 1 and pin diameter of 3 mm had the best thermal performance.	2018	[179]
Carbon foam paraffin wax(RT65)/nanocomposite	65 °C	Thermal control and protection of electronic devices.	The thermal management module is encapsulated in the aluminum support structure. The shell size is 50 mm × 50 mm × 40.5 mm and is processed with 1.2 mm thick aluminum.	Three different uniform power levels of 18, 24, 30 W	Experimental	Compared with pure carbon foam, the thermal management module composed of carbon foam + paraffin wax (RT65) was employed to achieve a reasonable delay in reaching the steady-state temperature of the heater.	2015	[180]
Carbon foam/PCM/nanocarbon tube composites	65 °C	Thermal management of electronic equipment	Thermal management module encapsulated in 1.5 mm thick thin aluminum shell	Pore values of different carbon foams (75%, 88%)	Numerical	When the porosity of foamed carbon was less than 75%, the module surface temperature decreased by 11.5%.	2015	[181]

Table 12. *Cont.*

PCM	Properties of PCM	Application	The Characteristics of Electronic Devices	Working Conditions	Research Method	Key Findings	Year	Reference
Paraffin (RT44HC)/expanded graphite (EG) composite PCM (CPCM)	41–44 °C	Li-ion battery thermal management	The commercial cylinder 26,650 $LiFePO_4$ battery	Dischargedat the rate of 5 C using a DC electronic load	Experimental	CPCM with 16–20 wt% expanded graphite can be regarded as the most promising alternative for Li-ion battery thermal management.	2016	[182]
Dielectric PCM-Boron Nitride Nanosheets Composite	-	Electronic system thermal management	-	Breakdown voltage 11.3–13.3 MV/m	Experimental	The thermal conductivity of the composite reached 3.47 W/(m·K), and the breakdown voltage reached 11.3–13.3 MV/m.	2016	[94]

Babapoor et al. [178] investigated the thermal management of a lithium-ion battery with carbon-fiber-based PCM (paraffin). The effects of the length and mass fraction of carbon fibers on the temperature profiles were studied. The experimental results showed that the thermal performance of PCMs mixed with 2-mm-long carbon fibers and 0.46% mass percentage was the best, and a 45% reduction of maximum temperature rise of the battery simulator could be achieved.

Wang et al. [176] studied the influence of paraffin/aluminum foam composite PCMs on Li-ion batteries by measuring the surface temperature of Li-ion batteries. The experimental results showed that foam composite PCMs had an ideal cooling effect in lowering the temperature rise of lithium-ion batteries during discharge. Results showed that the addition of composite PCMs decreased the highest temperature rise by 53%.

4.4. Other Applications

4.4.1. Telecommunications Cooling

Due to the necessity of 24 h uninterrupted operation of telecommunications base stations (TBs) and data centers (DC), the PCM–CTES system can meet its refrigeration needs in an emergency situation such as power failure, which will overcome the mismatch between energy supply and demand in time.

Sun et al. [183] proposed a technology using hydrated salt PCMs combined with a natural cold source, applied to TBs to decrease indoor temperature and to shorten the operation time of existing air conditioners. The PCT range of the selected PCM was 18–20 °C, the latent heat was 180 kJ/kg, and the thermal conductivity was 0.50 W/(m °C). The theoretical model was established through numerical simulation. The testing results of the latent heat storage unit (LHSU) showed that the average annual adjusted energy efficiency ratio was 14.04 W/W, which could be used effectively in TBs to reduce space cooling energy consumption.

Li et al. [184] adopted the genetic algorithm (GA) for performance optimization of their developed LHSU [183] and predicted the annual rate of four different climate zones in China. The results showed that the energy saving of Shenyang, Zhengzhou, Shenzhen, and Changsha could be improved by 6.48%, 4.39%, 3.48%, and 3.51%, respectively.

Wang et al. [185] took the air conditioning system transformation of a university DC as an example. A HP/vapor compression composite refrigeration device was built by adding a PCM-based CTES. The PCM selected in the scheme was solidified dodecanol–stearic acid composite materials, with a PCT of 20.2 °C and a latent heat of 201.2 kJ/kg. The results showed that the transformed air conditioning system could achieve 28% energy saving.

In order to reduce the cooling energy consumption of a traditional refrigeration system of DC and TBs, Chen et al. [186] designed a new refrigeration system based on PCM with six operation modes. The PCM used was a commercial inorganic material with a PCT range of 17–21 °C and a latent heat of 180 kJ/kg. This PCM was used to store the cooling capacity generated by outdoor air (OA) or vapor compression refrigeration (VCR) and for indoor cooling. The experimental results showed that the system could run smoothly, 14% higher than that of VCR when using OA charging.

Sundaram et al. [187] designed a passive cooling system combining PCM and a two-phase closed thermosyphon heat exchanger for telecommunications shelters in tropical and desert areas. The PCM used in the system was HS29 (commercial hydrated salt) with a PCT range of 28–30 °C and a latent heat of 205 kJ/kg. The PCM was used to store cooling capacity at night and to absorb the heat of electronic equipment during daytime operation. The passive cooling system could replace the traditional air conditioning system and save about 14 tons of carbon from the footprint every year.

4.4.2. LNG Cold Energy Utilization

Carbon dioxide liquefaction is carried out by the LNG cryogenic liquefaction process, i.e., using the low-temperature energy of LNG to cool the CO_2 with an intermediate coolant. Compared with the traditional absorption refrigerator process for cooling CO_2, it can

achieve remarkable energy saving effect. The Osaka Gas [188] upgraded the technology to make CO_2 gas and LNG directly contact and exchange heat to cool CO_2. This process reduces the power required for pressurization by 10%.

Zhao et al. [189] proposed a system to capture CO_2 in industrial exhaust gas by using LNG low-temperature energy. Taking the waste CO_2 discharged from the magnesite processing plant in Yingkou City, Liaoning Province, China, as the basic case of LNG cold energy recovery, the results showed the emission efficiency of 0.57, and 119.42 kW power and 0.75 tons of liquid CO_2 could be obtained per ton of LNG. The captured CO_2 can also be used as a raw material for chemical production.

Al-musleh et al. [190] proposed a process design of a solid oxide fuel cell power plant based on natural gas and CO_2 capture and liquefaction, referred to as an electrochemical refrigeration power plant. This process could achieve about 100% CO_2 capture and liquefaction, and the power generation efficiency was 70.4–76%.

Zhang et al. [191] introduced and compared two configurations of a new power generation system using LNG cold energy utilization and CO_2 capture. When the turbine inlet temperature was 900 °C, the output power of the two configurations were 51.6% and 59.1%, respectively, higher than that of commercial gas turbines at the same turbine inlet temperature.

All these examples showcase the promising application of PCM-based CTES systems in LNG cold energy valorization.

4.4.3. Fuel Cell Hydrogen Pressure Energy Recovery

Kim et al. [192] introduced a hydrogen pressure energy recovery system composed of hydrogen expander and PCM–CTES for fuel cell vehicles. The cold energy of expanded hydrogen was stored in the on-board PCM–CTES system and used to cool high-pressure hydrogen in the subsequent filling process. The PCM used was HS26N designed by savENRGIM. The Tm of the PCM was −25.6 °C, the Tf was −26.2 °C, and the latent heat was 205 kJ/kg. The system could reduce the energy loss of hydrogen in the process of energy conversion. The thermodynamic analysis results showed that when the expander efficiency was 0.53 and 1.0, the fuel efficiency could be increased by 1.39% and 2.63%, respectively.

5. Conclusions

With the extensive research activities on the material aspect of PCM in recent years (such as adding nanomaterials, microencapsulation, and shape stabilization), great technological progress has been achieved in the application of PCMs in CTES. Especially, the commercialized PCMs further promote the application of PCM–CTES in different fields. As mentioned above, PCM–CTES technology has been widely studied in building, refrigeration, thermal management of electronic equipment, and various other areas. In building, the application of PCM is divided into active and passive. The surveyed research proved that PCM integrated into buildings is beneficial, reducing the peak cooling load, the room temperature fluctuation, and the energy consumption. However, its disadvantage is that the incomplete solidification of PCM at night caused the inadequate use of PCMs. In refrigeration, PCM–CTES systems have been mainly used in cold chain transportation, food packaging and storage, household refrigerators, supermarket display cabinets, etc. Great prospects have been shown in refrigeration application, where the utilization of PCM reduces the compressor switching frequency, the energy consumption, and the operating cost. In the thermal management of electronic equipment, the application of PCM can effectively reduce the surface temperature rise of electronic equipment, reduce the battery surface temperature, and ensure the safety of electronic equipment [193]. With the increasing awareness of the importance of cold energy storage, the applications of PCM–CTES have also been expanded in various other fields. In addition to cold chain transportation and building free cooling, the research in emerging fields such as telecommunications cooling, supermarket, and large-scale industrial refrigeration are also increasing. The application of

PCMs in CTES can reduce the peak refrigeration demand. At the same time, the system can store cold at low electricity price at night to reduce the operation cost. Moreover, it can meet the cold energy demand in emergency and solve the mismatch between energy supply and user demand in time and space.

However, some challenges still remain to be overcome, as summarized below:

(1) Microencapsulation technology: the coating rate of cold storage PCM is low, and the selection of PCMs is limited (only applicable to organic PCMs).
(2) Although the addition of nanomaterials enhances the thermal conductivity of the composites, the latent heat of the composites is generally reduced, resulting in the decrease of energy storage capacity. Furthermore, the improvement of thermal conductivity also shortens the cooling release time, which is an inconvenience in cold chain transportation. Moreover, due to the higher cooling rate, the short crystal core formation time causes crystallization difficulties in the early stage of solidification, leading to the uneven internal heat transfer.
(3) The thermal performance decreases after multiple thawing cycles (such as the change of PCT and reduction of latent heat), which limits its long-term application in practice.
(4) Composite cold storage PCMs have high cost and poor practicability.
(5) There are few PCMs with PCT lower than −100 °C, and the corresponding research (such as for LNG cold energy utilization) is relatively lacking.

Considering the impact of cold storage PCMs on their efficiency, safety, cost, and feasibility, the following research directions could be considered in the future:

(1) Microencapsulation technology: optimize core and shell materials, and improve coating rate and thermal stability;
(2) Adding nanomaterials: appropriate nanomaterials and dosage to enhance the thermal conductivity without affecting the energy storage capacity;
(3) Problems such as supercooling and corrosion in the applications of PCMs remain to be solved;
(4) Design methods and standards for cold storage heat exchangers based on PCMs to improve the accurate control in the cooling process, and to avoid equipment frosting caused by supercooling;
(5) Explore more PCMs at lower temperature range with good thermal properties to meet the applications of CTES in more energy fields;
(6) Physical parameters of cold storage materials should be accurately measured and a complete database should be established to facilitate the practical applications of cold storage PCMs;
(7) When PCM–CTES is applied in building and refrigeration, the combination of active and passive strategies should be considered rather than a single strategy, so as to maximize the application potential of PCM–CTES.

Author Contributions: Conceptualization, X.Z., L.L. and Y.F.; methodology, Q.S. and X.Z.; formal analysis, Q.S., Q.W. and G.J.; investigation, Q.S., X.Z., Q.W. and G.J.; resources, X.Z. and L.L.; writing—original draft preparation, Q.S., Q.W. and G.J.; writing—review and editing, X.Z., Q.S., L.L., Y.F., Q.W. and G.J.; supervision, X.Z.; project administration, X.Z.; funding acquisition, X.Z. and L.L. All authors have read and agreed to the published version of the manuscript.

Funding: This research was funded by Key Research and Development (R&D) Projects of Shanxi Province grant number [201803D31035] and by European project H2020-MSCA-RISE-2016: Low Energy Dew Point Cooling for Computing Data Centers (DEW-COOL-4CDC).

Institutional Review Board Statement: Not applicable.

Informed Consent Statement: Not applicable.

Acknowledgments: This work is supported by the Key Research and Development (R&D) Projects of Shanxi Province (201803D31035) and European project H2020-MSCA-RISE-2016: Low Energy Dew Point Cooling for Computing Data Centers (DEW-COOL-4CDC).

Conflicts of Interest: The authors declare no conflict of interest.

References

1. National Development and Reform Commission. Green and Efficient Refrigeration Action Plan. 2019. Available online: https://www.ndrc.gov.cn/ (accessed on 1 September 2021).
2. Dardir, M.; Panchabikesan, K.; Haghighat, F.; El Mankibi, M.; Yuan, Y. Opportunities and challenges of PCM-to-air heat exchangers (PAHXs) for building free cooling applications—A comprehensive review. *J. Energy Storage* **2019**, *22*, 157–175. [CrossRef]
3. Iten, M.; Liu, S.; Shukla, A. A review on the air-PCM-TES application for free cooling and heating in the buildings. *Renew. Sustain. Energy Rev.* **2016**, *61*, 175–186. [CrossRef]
4. Alizadeh, M.; Sadrameli, S. Development of free cooling based ventilation technology for buildings: Thermal energy storage (TES) unit, performance enhancement techniques and design considerations—A review. *Renew. Sustain. Energy Rev.* **2016**, *58*, 619–645. [CrossRef]
5. Souayfane, F.; Fardoun, F.; Biwole, P.-H. Phase change materials (PCM) for cooling applications in buildings: A review. *Energy Build.* **2016**, *129*, 396–431. [CrossRef]
6. Faraj, K.; Khaled, M.; Faraj, J.; Hachem, F.; Castelain, C. Phase change material thermal energy storage systems for cooling applications in buildings: A review. *Renew. Sustain. Energy Rev.* **2019**, *119*, 109579. [CrossRef]
7. Akeiber, H.; Nejat, P.; Majid, M.Z.A.; Wahid, M.A.; Jomehzadeh, F.; Famileh, I.Z.; Calautit, J.K.; Hughes, B.R.; Zaki, S.A. A review on phase change material (PCM) for sustainable passive cooling in building envelopes. *Renew. Sustain. Energy Rev.* **2016**, *60*, 1470–1497. [CrossRef]
8. Romdhane, S.B.; Amamou, A.; Rim, B.K.; Nejla, M.S.; Zohir, Y.; Abdelmajid, J. A review on thermal energy storage using phase change materials in passive building applications. *J. Build. Eng.* **2020**, *32*, 101563. [CrossRef]
9. Waqas, A.; Din, Z.U. Phase change material (PCM) storage for free cooling of buildings—A review. *Renew. Sustain. Energy Rev.* **2013**, *18*, 607–625. [CrossRef]
10. Li, S.F.; Liu, Z.H.; Wang, X.J. A comprehensive review on positive cold energy storage technologies and applications in air conditioning with phase change materials. *Appl. Energy* **2019**, *255*, 113667. [CrossRef]
11. Raj, V.A.A.; Velraj, R. Review on free cooling of buildings using phase change materials. *Renew. Sustain. Energy Rev.* **2010**, *14*, 2819–2829. [CrossRef]
12. Sharma, R.K.; Ganesan, P.; Tyagi, V.V.; Metselaar, H.S.C.; Sandaran, S.C. Developments in organic solid–liquid phase change materials and their applications in thermal energy storage. *Energy Convers. Manag.* **2015**, *95*, 193–228. [CrossRef]
13. Kalnaes, S.E.; Jelle, B.P. Phase change materials and products for building applications: A state-of-the-art review and future research opportunities. *Energy Build.* **2015**, *94*, 150–176. [CrossRef]
14. Zheng, L.; Zhang, W.; Liang, F. A review about phase change material cold storage system applied to solar-powered air-conditioning system. *Adv. Mech. Eng.* **2017**, *9*, 1–20. [CrossRef]
15. Zhai, X.Q.; Wang, X.L.; Wang, T.; Wang, R.Z. A review on phase change cold storage in air-conditioning system: Materials and applications. *Renew. Sustain. Energy Rev.* **2013**, *22*, 108–120. [CrossRef]
16. Osterman, E.; Tyagi, V.V.; Butala, V.; Rahim, N.A.; Stritih, U. Review of PCM based cooling technologies for buildings. *Energy Build.* **2012**, *49*, 37–49. [CrossRef]
17. Gang, L.; Hwang, Y.; Radermacher, R. Review of cold storage materials for air conditioning application—ScienceDirect. *Int. J. Refrig.* **2012**, *35*, 2053–2077.
18. Sidik, N.A.C.; Kean, T.H.; Chow, H.K.; Rajaandra, A.; Rahman, S.; Kaur, J. Performance enhancement of cold thermal energy storage system using nanofluid phase change materials: A review. *Int. Commun. Heat Mass Transf.* **2018**, *94*, 85–95. [CrossRef]
19. Ali, H.M. Applications of combined/hybrid use of heat pipe and phase change materials in energy storage and cooling systems: A recent review. *J. Energy Storage* **2019**, *26*, 100986. [CrossRef]
20. Kibria, M.A.; Anisur, M.R.; Mahfuz, M.H.; Saidur, R.; Metselaar, I.H.S.C. A review on thermophysical properties of nanoparticle dispersed phase change materials. *Energy Convers. Manag.* **2015**, *95*, 69–89. [CrossRef]
21. Joybari, M.M.; Haghighat, F.; Moffat, J.; Sra, P. Heat and cold storage using phase change materials in domestic refrigeration systems: The state-of-the-art review. *Energy Build.* **2015**, *106*, 111–124. [CrossRef]
22. Selvnes, H.; Allouche, Y.; Manescu, R.I.; Hafner, A. Review on cold thermal energy storage applied to refrigeration systems using phase change materials. *Therm. Sci. Eng. Prog.* **2020**, *22*, 100807. [CrossRef]
23. Nie, B.; Palacios, A.; Zou, B.; Liu, J.; Zhang, T.; Li, Y. Review on phase change materials for cold thermal energy storage applications. *Renew. Sustain. Energy Rev.* **2020**, *134*, 110340. [CrossRef]
24. Oró, E.; De Gracia, A.; Castell, A.; Farid, M.M.; Cabeza, L.F. Review on phase change materials (PCMs) for cold thermal energy storage applications. *Appl. Energy* **2012**, *99*, 513–533. [CrossRef]
25. Li, G.; Hwang, Y.; Radermacher, R.; Chun, H.-H. Review of cold storage materials for subzero applications. *Energy* **2013**, *51*, 1–17. [CrossRef]
26. Yang, L.; Villalobos, U.; Akhmetov, B.; Gil, A.; Khor, J.O.; Palacios, A.; Li, Y.; Ding, Y.; Cabeza, L.F.; Tan, W.L.; et al. A comprehensive review on sub-zero temperature cold thermal energy storage materials, technologies, and applications: State of the art and recent developments. *Appl. Energy* **2021**, *288*, 116555. [CrossRef]

27. Tatsidjodoung, P.; Le Pierrès, N.; Luo, L. A review of potential materials for thermal energy storage in building applications. *Renew. Sustain. Energy Rev.* **2013**, *18*, 327–349. [CrossRef]
28. Cabeza, L.F.; Castell, A.; Barreneche, C.; De Gracia, A.; Fernández, A.I. Materials used as PCM in thermal energy storage in buildings: A review. *Renew. Sustain. Energy Rev.* **2011**, *15*, 1675–1695. [CrossRef]
29. Huang, Y.; Zhang, X.L.; Yang, Y.; Yuan, Y. Preparation and Thermal Performance of the Phase Change Storage Materials for Refrigerated Transport. *J. Refrig. Technol.* **2014**, *4*, 14–17.
30. Yibo, F.U.; Dongmei, W.; Hong, Z. Review on Low Temperature Phase Change Materials and Its Application. *Mater. Rev.* **2016**, *30*, 222–226.
31. Yang, T.R.; Sun, Q.; Wennersten, R.; Cheng, L. Review of Phase Change Materials for Cold Thermal Energy Storage. *K. Cheng Je Wu Li Hsueh Pao/J. Eng. Thermophys.* **2018**, *39*, 567–573.
32. Yongsheng, Y.U.; Qiangshan, J.; Yaqian, S. Progress in studies of low temperature phase-change energy storage materials. *Chem. Ind. Eng. Prog.* **2010**, *29*, 896–900.
33. Borri, E.; Sze, J.Y.; Tafone, A.; Romagnoli, A.; Li, Y.; Comodi, G. Experimental and numerical characterization of sub-zero phase change materials for cold thermal energy storage. *Appl. Energy* **2020**, *275*, 115131. [CrossRef]
34. Sharma, S.D. Phase Change Materials for Low Temperature Solar Thermal Applications. *Res. Rep. Fac. Eng. Mie Univ.* **2004**, *29*, 31–64.
35. Li, X.Y.; Yang, L.; Wang, X.L.; Miao, X.Y.; Yao, Y.; Qiang, Q.Q. Investigation on the charging process of a multi-PCM latent heat thermal energy storage unit for use in conventional air-conditioning systems. *Energy* **2018**, *150*, 591–600. [CrossRef]
36. Veerakumar, C.; Sreekumar, A. Phase change material based cold thermal energy storage: Materials, techniques and applications—A review. *Int. J. Refrig.* **2016**, *67*, 271–289. [CrossRef]
37. Fu, L.L.; Jiang, D.G.; Zhou, C.Y. Determination of Thermodynamic Parameters of Isopropyl Palmitate Synthesis. *J. Chem. Engine Ering Chin. Universties* **2017**, *31*, 733–737.
38. Pielichowska, K.; Pielichowski, K. Phase change materials for thermal energy storage. *Prog. Mater. Sci.* **2014**, *65*, 67–123. [CrossRef]
39. Gasanaliev, A.M.; Gamataeva, B.Y. Heat-accumulating properties of melts. *Russ. Chem. Rev.* **2000**, *69*, 192–200. [CrossRef]
40. Noro, M.; Lazzarin, R.; Busato, F. Solar cooling and heating plants: An energy and economic analysis of liquid sensible vs. phase change material (PCM) heat storage. *Int. J. Refrig.* **2014**, *39*, 104–116. [CrossRef]
41. Fang, M.T.; Zhang, X.L.; Ji, J.; Hua, W.S.; Liu, B.; Wang, X.Z. Progress in hydrated salt based composite phase change materials. *Energy Storage Sci. Technol.* **2019**, *8*, 709–717.
42. Baetens, R.; Jelle, B.P.; Gustavsen, A. Phase change materials for building applications: A state-of-the-art review. *Energy Build.* **2010**, *42*, 1361–1368. [CrossRef]
43. Haghighat, F. Applying energy storage in ultra-low energy buildings. *IEA Annex* **2013**, *23*, 834–835.
44. Xing-Ren, L.I.; Ming-Wei, T.; Bi-Rong, W.U. Experiments on the eutectic salt used as low temperature cool storage material. *J. Chongqing Univ.* **2004**, *8*, 113–115.
45. Gunasekara, S.N.; Kumova, S.; Chiu, J.N.W.; Martin, V. Experimental phase diagram of the dodecane–tridecane system as phase change material in cold storage. *Int. J. Refrig.* **2017**, *82*, 130–140. [CrossRef]
46. Li, Y.; Guo, Y.F.; Fu, J.; Liang, J. Preparation and thermophysical performance of organic phase change energy storage materials in cold chain transportation. *Acta Mater. Compos. Sin.* **2022**, in press.
47. Bo, H.; Gustafsson, E.; Setterwall, F. Tetradecane and hexadecane binary mixtures as phase change materials (PCMs) for cool storage in district cooling systems. *Energy* **1999**, *24*, 1015–1028. [CrossRef]
48. Zhang, X.L.; Chen, Y.F.; Zeng, T.; Lv, W. Research and development of phase change materials for pharmaceutical cold chain logistics. *Refrig. Air-Cond.* **2017**, *17*, 43–46.
49. Shengli, T.; Dong, Z.; Deyan, X. Experimental study of caprylic acid/lauric acid molecular alloys used as low-temperature phase change materials in energy storage. *Energy Conserv.* **2005**, *6*, 45–47.
50. Zhao, Y.; Zhang, X.; Xu, X.; Zhang, S. Development of composite phase change cold storage material and its application in vaccine cold storage equipment. *J. Energy Storage* **2020**, *30*, 101455. [CrossRef]
51. Bo, H.; Setterwall, F. Technical grade paraffin waxes as phase change materials for cool thermal storage and cool storage systems capital cost estimation. *Energy Convers. Manag.* **2002**, *43*, 1709–1723.
52. Gao, H.T. Investigation on organic phase transition materials in Energy Storage Air Conditioning system. In Proceedings of the 2011 International Conference on Materials for Renewable Energy & Environment, Shanghai, China, 20–22 May 2011.
53. Zuo, J.; Li, W.; Weng, L. Thermal performance of caprylic acid/1-dodecanol eutectic mixture as phase change material (PCM). *Energy Build.* **2011**, *43*, 207–210. [CrossRef]
54. Xing, L.; Fang, G.Y.; Yang, F. Preparation and Thermal Performance Analysis of Cold Storage Material for Air Conditioning System. *China Appl. Technol.* **2006**, *3*, 47–48.
55. Wu, W.; Tang, H.; Miao, P.; Zhang, H. Preparation and thermal properties of nano-organic composite phase change materials for cool storage in air-conditioning. *CIESC J.* **2015**, *66*, 1208–1214.
56. Xiao-Cai, H.U.; Hui-Jun, W.U.; Zhou, X.Q. Crystallizing characteristics of binary mixtures of Dodecanol/Caprylic acid for phase change cool storage. *J. Guangzhou Univ.* **2011**, *10*, 60–63.
57. Hussain, S.I.; Dinesh, R.; Roseline, A.A.; Dhivya, S.; Kalaiselvam, S. Enhanced thermal performance and study the influence of sub cooling on activated carbon dispersed eutectic PCM for cold storage applications. *Energy Build.* **2017**, *143*, 17–24. [CrossRef]

58. Dimaano, M.N.R.; Watanabe, T. The capric–lauric acid and pentadecane combination as phase change material for cooling applications. *Appl. Therm. Eng.* **2002**, *22*, 365–377. [CrossRef]
59. Roxas-Dimaano, M.N.; Watanabe, T. The capric and lauric acid mixture with chemical additives as latent heat storage materials for cooling application. *Energy* **2002**, *27*, 869–888. [CrossRef]
60. Jia, X.; Zhai, X.; Cheng, X. Thermal performance analysis and optimization of a spherical PCM capsule with pin-fins for cold storage. *Appl. Therm. Eng.* **2018**, *148*, 929–938. [CrossRef]
61. Kumar, R.; Vyas, S.; Dixit, A. Fatty acids/1-dodecanol binary eutectic phase change materials for low temperature solar thermal applications: Design, development and thermal analysis. *Sol. Energy* **2017**, *155*, 1373–1379. [CrossRef]
62. Philip, N.; Dheep, G.R.; Sreekumar, A. Cold thermal energy storage with lauryl alcohol and cetyl alcohol eutectic mixture: Thermophysical studies and experimental investigation. *J. Energy Storage* **2020**, *27*, 101060. [CrossRef]
63. Jebasingh, B.E.; Arasu, A.V. Characterisation and stability analysis of eutectic fatty acid as a low cost cold energy storage phase change material. *J. Energy Storage* **2020**, *31*, 101708. [CrossRef]
64. Yang, Y.Y.; Fu, S.Y.; Wu, W.D.; Zhang, D. Preparation and performance evaluation of a new type of binary shaped phase change material for buildings. *Chem. Ind. Eng. Prog.* **2020**, *39*, 4119–4126.
65. Chinnasamy, V.; Appukuttan, S. Preparation and thermal properties of lauric acid/myristyl alcohol as a novel binary eutectic phase change material for indoor thermal comfort. *Energy Storage* **2019**, *1*, e80. [CrossRef]
66. Sarı, A.; Karaipekli, A. Preparation and thermal properties of capric acid/palmitic acid eutectic mixture as a phase change energy storage material. *Mater. Lett.* **2008**, *62*, 903–906. [CrossRef]
67. Chinnasamy, V.; Sreekumar, A. Preparation, Thermophysical Studies, and Corrosion Analysis of a Stable Capric Acid/Cetyl Alcohol Binary Eutectic Phase Change Material for Cold Thermal Energy Storage. *Energy Technol.* **2018**, *6*, 397–405.
68. Jarrar, R.; Sawafta, R. Binary and Ternary Mixtures of Eicosane with Fatty Alcohols and Fatty Acids as Phase Change Material for Building Applications. *Palest. Tech. Univ. Res. J.* **2018**, *6*, 16–22. [CrossRef]
69. Saeed, R.M.; Schlegel, J.P.; Castano, C.; Sawafta, R.; Kuturu, V. Preparation and thermal performance of methyl palmitate and lauric acid eutectic mixture as phase change material (PCM). *J. Energy Storage* **2017**, *13*, 418–424. [CrossRef]
70. Shen, J.; Hu, Z.; Wang, C.; Chen, K.; Cai, Z.; Wang, T. Preparation and Thermal Properties of Stearic Acid/n-Octadecane Binary Eutectic Mixture as Phase Change Materials for Energy Storage. *ChemistrySelect* **2019**, *4*, 4125–4130. [CrossRef]
71. Zheng, D.X.; Wu, X.H. Comprehensive evaluation eutectic character used as low temperature thermal energy storage. *Cryogenics* **2002**, *1*, 37–45.
72. Sun, Z.G.; Jiang, C.M.; Sun, L. Experiment on Phase Change Conditions and Phase Change Latent Heat of Tetra-n-butyl Ammonium Bromide Aqueous Solutions for Cold Storage. *J. Refrig.* **2009**, *30*, 24–26.
73. Zhang, M.; Fang, G.Y.; Wu, S.M.; Yang, F. Experimental Study on Thermal Characteristics of Phase-change Material Tetra-n-butylammonium Bromide for Cool Storage. *J. Refrig.* **2008**, *5*, 8–11.
74. Liu, J.H.; Liu, R.H.; Wang, C.H.; Liang, Y.N. Thermodynamics test of Na_2SO_4·10H_2O phase change compound system. *Energy Conserv.* **2007**, *9*, 13–14.
75. Available online: https://www.pcmproducts.net/Eutectic_Refrigeration_PCMs.htm (accessed on 1 September 2021).
76. Available online: www.teapcm.com (accessed on 1 September 2021).
77. Available online: www.cristopia.com (accessed on 1 September 2021).
78. Available online: www.microteklabs.com (accessed on 1 September 2021).
79. Kakiuchi, H. *Mitsubishi Chemical*; Mitsubishi Chemical Corporation: Tokyo, Japan, 2002.
80. Available online: www.climator.com (accessed on 1 September 2021).
81. Available online: www.rubitherm.eu (accessed on 1 September 2021).
82. Available online: www.puretemp.com (accessed on 1 September 2021).
83. Available online: www.epsltd.co (accessed on 1 September 2021).
84. Wang, X.; Ding, Q.; Yao, X.L.; Fang, X.; Fan, L.W.; Xu, X.; Yu, Z.T.; Hu, Y.C. Thermophysical properties of paraffin-based composite phase change materials filled with carbon nanotubes. *J. Therm. Ence Technol.* **2013**, *12*, 124–130.
85. Puyue, J.; Weidong, W.U.; Yicong, W. Preparation of 0°C phase change material and its cold storage performance in cold-chain logistics. *Chem. Ind. Eng. Prog.* **2019**, *38*, 2862–2869.
86. Zhang, X.L.; Zhou, S.X.; Liu, S.; Li, Y.Y.; Xu, X.F.; Wang, Y.H.; Liu, L. Cold Storage Characteristics of n-Octanoic-Lauric Acid Nanocomposite Phase Change Materials. *Tianjin Daxue Xuebao/J. Tianjin Univ. Ence Technol.* **2019**, *52*, 71–77.
87. Yudong, L.; Xin, L.I. Cold Charge and Discharge Characteristics of Nanofluids and Its Application to Ice Storage Using Valley Electricity. *Zhongguo Dianji Gongcheng Xuebao/Proc. Chin. Soc. Electr. Eng.* **2015**, *35*, 2779–2787.
88. Liu, Y.D. Study on Preparation and Thermal Properties of Phase Change Nanocomposites for Cool Storage. Ph.D. Thesis, Chongqing University, Chongqing, China, 2005.
89. Sathishkumar, A.; Kumaresan, V.; Velraj, R. Solidification characteristics of water based graphene nanofluid PCM in a spherical capsule for cool thermal energy storage applications. *Int. J. Refrig.* **2016**, *66*, 73–83. [CrossRef]
90. Sun, J.P.; Zhou, X.Q.; Wu, H.J. Experimental Study on the Performance of Organic Phase-Change Cold Storage Material with Carbon Nanotube Additives. *Chem. Ind. Times* **2012**, *26*, 9–13.
91. Xiao-Yan, L.I.; Yan, W.; Jing-Yu, Z. Study on heat transfer properties with phase change nanocomposites in air-conditioning system. *J. Harbin Univ. Commer.* **2008**, *2008 24*, 738–740.

92. Xiao-Yan, L.I. Study of new cool storage materials for air conditioning cool storage system. *Appl. ENCE Technol.* **2004**, *7*, 66–68.
93. Wu, X.H.; Wang, C.X.; Gao, M.T.; Li, W.P. Experimental Study of Thermo-physical Properties of Paraffin-Carbon Nanotubes Composite Materials. *J. Eng. Thermophys.* **2017**, *38*, 1071–1076.
94. Zhi, Y.; Zhou, L.; Wei, L.; Wan, J.; Dai, J.; Han, X.; Fu, K.; Henderson, D.; Bao, Y.; Hu, L. Thermally Conductive, Dielectric PCM-Boron Nitride Nanosheets Composite for Efficient Electronic System Thermal Management. *Nanoscale* **2016**, *8*, 19326–19333.
95. Huang, Y.; She, X.; Li, C.; Li, Y.; Ding, Y. Evaluation of thermal performance in cold storage applications using EG-water based nano-composite PCMs. *Energy Procedia* **2019**, *158*, 4840–4845. [CrossRef]
96. Hao, M.; Li, Z.H.; Wu, Q.F.; Gao, W.; Ma, X.S. Research progress of encapsulation technology for phase change materials. *Mater. Rev.* **2014**, *28*, 98–103.
97. Jurkowska, M.; Szczygieł, I. Review on properties of microencapsulated phase change materials slurries (mPCMS). *Appl. Therm. Eng.* **2016**, *98*, 365–373. [CrossRef]
98. Xu, B.; Li, P.; Chan, C. Application of phase change materials for thermal energy storage in concentrated solar thermal power plants: A review to recent developments. *Appl. Energy* **2015**, *160*, 286–307. [CrossRef]
99. Jelle, B.P.; Kalnæs, S.E. Phase Change Materials for Application in Energy-Efficient Buildings. In *Cost-Effective Energy Efficient Building Retrofitting Materials, Technologies, Optimization and Case Studies*; Elsevier: Amsterdam, The Netherlands, 2017; pp. 57–118. [CrossRef]
100. Giro-Paloma, J.; Martínez, M.; Cabeza, L.F.; Fernández, A.I. Types, methods, techniques, and applications for microencapsulated phase change materials (MPCM): A review. *Renew. Sustain. Energy Rev.* **2016**, *53*, 1059–1075. [CrossRef]
101. Lin, X.; Gui-Yin, F.; Fan, Y. Study on the preparation and performance of the microcapsule phase change material for cool storage. *Vac. Cryog.* **2006**, *3*, 153–156.
102. Xu, H.; Yang, R.; Zhang, Y.P. A Microencapsulated Phase Change Refrigerant for Air Conditioning Storage and Its Preparation. Method. Patent CN1621483.2005-06-01, 1 June 2005.
103. Dai, X.; Sheng, X. Study on Preparation of Heat Insulation Micropcms for Blood. *Mater. Rev.* **2007**, *S1*, 361–363.
104. Yu, S.; Wang, X.; Wu, D. Microencapsulation of n-octadecane phase change material with calcium carbonate shell for enhancement of thermal conductivity and serving durability: Synthesis, microstructure, and performance evaluation. *Appl. Energy* **2014**, *114*, 632–643. [CrossRef]
105. Wang, T.; Wang, S.; Luo, R.; Zhu, C.; Akiyama, T.; Zhang, Z. Microencapsulation of phase change materials with binary cores and calcium carbonate shell for thermal energy storage. *Appl. Energy* **2016**, *171*, 113–119. [CrossRef]
106. You, M. *Preparation of Microencapsulated Phase Change Materials and Its Application in Polyurethane Foam*; Tianjin Polytechnic University: Tianjin, China, 2010. [CrossRef]
107. Yu, D.W. *Preparation and Performance Optimization Research of Microencapsulated Phase Change Materials with Refrigeration Temperature Control Packaging*; Southern Yangtze University: Wuxi, China, 2015.
108. Fu, W.; Liang, X.; Xie, H.; Wang, S.; Gao, X.; Zhang, Z.; Fang, Y. Thermophysical properties of n -tetradecane@polystyrene-silica composite nanoencapsulated phase change material slurry for cold energy storage. *Energy Build.* **2017**, *136*, 26–32. [CrossRef]
109. Tumirah, K.; Hussein, M.Z.; Zulkarnain, Z.; Rafeadah, R. Nano-encapsulated organic phase change material based on copolymer nanocomposites for thermal energy storage. *Energy* **2014**, *66*, 881–890. [CrossRef]
110. Qian, T.; Li, J.; Ma, H.; Yang, J. The preparation of a green shape-stabilized composite phase change material of polyethylene glycol/SiO2 with enhanced thermal performance based on oil shale ash via temperature-assisted sol–gel method. *Sol. Energy Mater. Sol. Cells* **2015**, *132*, 29–39. [CrossRef]
111. Fang, Y.; Kuang, S.; Gao, X.; Zhang, Z. Preparation and Characterization of Novel Nanoencapsulated Phase Change Materials. *Energy Convers. Manag.* **2008**, *49*, 3704–3707. [CrossRef]
112. Wang, X.; Zhang, L.; Yu, Y.-H.; Jia, L.; Mannan, M.S.; Chen, Y.; Cheng, Z. Nano-encapsulated PCM via Pickering Emulsification. *Sci. Rep.* **2015**, *5*, 13357. [CrossRef]
113. Yu, Q.; Tchuenbou-Magaia, F.; Al-Duri, B.; Zhang, Z.; Ding, Y.; Li, Y. Thermo-mechanical analysis of microcapsules containing phase change materials for cold storage. *Appl. Energy* **2018**, *211*, 1190–1202. [CrossRef]
114. Jiang, S.; Yu, D.; Ji, X.; An, L.; Jiang, B. Confined crystallization behavior of PEO in silica networks. *Polymer* **2000**, *41*, 2041–2046. [CrossRef]
115. Jiang, Y.; Ding, E.; Li, G. Study on transition characteristics of PEG/CDA solid–solid phase change materials. *Polymer* **2002**, *43*, 117–122. [CrossRef]
116. Pielichowski, K.; Flejtuch, K. Thermal properties of poly(ethylene oxide)/lauric acid blends: A SSA–DSC study. *Thermochim. Acta* **2006**, *442*, 18–24. [CrossRef]
117. Py, X.; Olives, R.; Mauran, S. Paraffin/porous-graphite-matrix composite as a high and constant power thermal storage material. *Int. J. Heat Mass Transf.* **2001**, *44*, 2727–2737. [CrossRef]
118. Xu, X.F.; Zhang, X.L.; Munyalo, J.M. Key technologies and research progress on enhanced characteristics of cold thermal energy storage. *J. Mol. Liq.* **2019**, *278*, 428–437. [CrossRef]
119. Zhang, X.X.; Shu-Qin, L.I.; Chen, S.; Pei, D.F. Preparation and characterization of poly(diethylene glycol hexadecyl ether acrylate)/graphene oxide composite shape- stabilized phase change materials. *J. Tianjin Polytech. Univ.* **2016**, *35*, 1–6.
120. Xiaolin, W.U.; Zhang, H.; Zou, J.; Sun, R. Structural and Thermo-physical Analysis of Polyurethane Form-stable Phase Change Energy Storage Materials. *Mater. Rev.* **2012**, *26*, 94–97.

121. Ma, F.; Wang, X.Y.; Cheng, L.Y. Study on preparation and properties of capric acid-lauric acid/expanded graphite phase change materials. *J. Funct. Mater.* **2010**, *41*, 180–183.
122. Leng, C.B. *Preparation and Performance Analysis of Expanded Graphite/Hydrated Salt Composite Shape-stabilized Phase Change Material*; Yunnan Normal University: Kunming, China, 2015.
123. Liu, J.S.; Jia-Jing, M.; Zhang, J.; Yang, H.L.; Feng, B.; Jiang, K.; Li, X.; Liu, H.K.; Wen, J.H. Study on the preparation and poperties of lauric acidexpanded perlite composite phase change materials. *J. Wuhan Polytech. Univ.* **2014**, *33*, 82–84.
124. Wu, F.C. *Preparation of the Ss-PCMs and Experiemtal Study in the Thermal Characteristic of PCM Room Model*; Chongqing University: Chongqing, China, 2010.
125. Feng, L.L.; Zheng, J.; Yang, H.Z.; Guo, Y.L.; Li, W.; Li, X.G. Preparation and characterization of polyethylene glycol/active carbon composites as shape-stabilized phase change materials—ScienceDirect. *Sol. Energy Mater. Sol. Cells* **2011**, *95*, 644–650. [CrossRef]
126. Sun, Z.; Kong, W.; Zheng, S.; Frost, R.L. Study on preparation and thermal energy storage properties of binary paraffin blends/opal shape-stabilized phase change materials. *Sol. Energy Mater. Sol. Cells* **2013**, *117*, 400–407. [CrossRef]
127. Sar, A.; Karaipekli, A. Preparation, thermal properties and thermal reliability of capric acid/expanded perlite composite for thermal energy storage. *Mater. Chem. Phys.* **2008**, *109*, 459–464. [CrossRef]
128. Feng, L.P.; Wang, M. Preparation of shaped phase change cool storage paraffin based materials with different supports. *New Chem. Mater.* **2020**, *48*, 140–142.
129. Song, Y.; Zhang, N.; Jing, Y.; Cao, X.; Yuan, Y.; Haghighat, F. Experimental and numerical investigation on dodecane/expanded graphite shape-stabilized phase change material for cold energy storage. *Energy* **2019**, *189*, 116175. [CrossRef]
130. Ying, Y.; Shen, H.-Y. Investigation on cryogenics cool thermal energy storage phase change composition material. *Chin. J. Low Temp. Phys.* **2009**, *31*, 144–147.
131. Yan, H.; Xue-Lai, Z. Research of Composite Cool Storage Materials for Cold Chain Logistics. *Chin. J. Refrig. Technol.* **2016**, *36*, 12–15.
132. Wang, H.; Liu, Z.B.; Zhao, Y. Frozen Properties of Phase Change Cool Storage Materials in the Refrigerator Freezer. *Refrig. Air Cond.* **2015**, *29*, 6–10.
133. Lu, W.; Liu, G.; Xing, X.; Wang, H. Investigation on Ternary Salt-Water Solutions as Phase Change Materials for Cold Storage. *Energy Procedia* **2019**, *158*, 5020–5025. [CrossRef]
134. Ravikumar, M.; Srinivasan, P. Phase change material as thermal energy storage material for cooling of buildings. *J. Theor. Appl. Inf. Technol.* **2008**, *4*, 503–511.
135. ASHRAE. *ANSI-ASHRAE 55a-1995, Addendum to ANSI-ASHRAE Standard 55-1992, Thermal Environmental Conditions for Human Occupancy*; American Society of Heating, Refrigerating and Air Conditioning Engineers, Atlanta, Inc.: Atlanta, GA, USA, 1995.
136. Turnpenny, J.R.; Etheridge, D.W.; Reay, D.A. Novel ventilation system for reducing air conditioning in buildings. Part II: Testing of prototype. *Appl. Therm. Eng.* **2001**, *21*, 1203–1217. [CrossRef]
137. Nagano, K.; Takeda, S.; Mochida, T.; Shimakura, K. Thermal characteristics of a direct heat exchange system between granules with phase change material and air. *Appl. Therm. Eng.* **2004**, *24*, 2131–2144. [CrossRef]
138. Alessandro, M.; Göran, H.; Bergsøe, N.C.; Alireza, A. Free cooling potential of a PCM-based heat exchanger coupled with a novel HVAC system for simultaneous heating and cooling of buildings. *Sustain. Cities Soc.* **2018**, *42*, 384–395.
139. Piselli, C.; Prabhakar, M.; de Gracia, A.; Saffari, M.; Pisello, A.L.; Cabeza, L.F. Optimal control of natural ventilation as passive cooling strategy for improving the energy performance of building envelope with PCM integration. *Renew. Energy* **2020**, *162*, 171–181. [CrossRef]
140. Philip, N.; Veerakumar, C.; Sreekumar, A. Lauryl alcohol and stearyl alcohol eutectic for cold thermal energy storage in buildings: Preparation, thermophysical studies and performance analysis. *J. Energy Storage* **2020**, *31*, 101600. [CrossRef]
141. Ruevskis, S.; Akishin, P.; Korjakins, A. Parametric analysis and design optimisation of PCM thermal energy storage system for space cooling of buildings—ScienceDirect. *Energy Build.* **2020**, *224*, 110288. [CrossRef]
142. Kong, X.F.; Yao, C.Q.; Jie, P.F.; Liu, Y.; Qi, C.Y.; Rong, X. Development and thermal performance of an expanded perlite-based phase change material wallboard for passive cooling in building. *Energy Build.* **2017**, *152*, 547–557. [CrossRef]
143. Gholamibozanjani, G.; Farid, M. Application of an active PCM storage system into a building for heating/cooling load reduction. *Energy* **2020**, *210*, 118572. [CrossRef]
144. Yu, H.; Li, C.E.; Zhang, K.G.; Tang, Y.; Song, Y.; Wang, M. Preparation and Thermophysical Performance of Diatomite-Based Composite PCM Wallboard for Thermal Energy Storage in Buildings. *J. Build. Eng.* **2020**, *32*, 101753. [CrossRef]
145. Chen, X.; Zhang, Q.; Zhai, Z.J.; Ma, X. Potential of ventilation systems with thermal energy storage using PCMs applied to air conditioned buildings. *Renew. Energy* **2019**, *138*, 39–53. [CrossRef]
146. Maleki, B.; Khadang, A.; Maddah, H.; Alizadeh, M.; Kazemian, A.; Ali, H.M. Development and thermal performance of nanoencapsulated PCM/plaster wallboard for thermal energy storage in buildings. *J. Build. Eng.* **2020**, *32*, 101727. [CrossRef]
147. Guarino, F.; Dermardiros, V.; Chen, Y.; Rao, J.; Athienitis, A.; Cellura, M.; Mistretta, M. PCM Thermal Energy Storage in Buildings: Experimental Study and Applications. *Energy Procedia* **2015**, *70*, 219–228. [CrossRef]
148. Chen, X.; Zhang, Q.; Zhai, Z.; Qiu, J. Performance of a cold storage air-cooled heat pump system with phase change materials for space cooling. *Energy Build.* **2020**, *228*, 110405. [CrossRef]
149. Ezan, M.A.; Doganay, E.O.; Yavuz, F.E.; Tavman, I.H. A numerical study on the usage of phase change material (PCM) to prolong compressor off period in a beverage cooler. *Energy Convers. Manag.* **2017**, *142*, 95–106. [CrossRef]

150. Du, J.; Nie, B.; Zhang, Y.; Du, Z.; Wang, L.; Ding, Y. Cooling performance of a thermal energy storage-based portable box for cold chain applications. *J. Energy Storage* **2020**, *28*, 101238. [CrossRef]
151. Ghahramani, Z.O.; Rouhollah, A. Employment of Finned PCM Container in a Household Refrigerator as a Cold Thermal Energy Storage System. *Therm. Sci. Eng. Prog.* **2018**, *7*, 115–124. [CrossRef]
152. Tian, S.; Yang, Q.F.; Hui, N.; Bai, H.Z.; Shao, S.Q.; Liu, S.C. Discharging process and performance of a portable cold thermal energy storage panel driven by embedded heat pipes. *Energy* **2020**, *205*, 117987. [CrossRef]
153. Ben-Abdallah, R.; Leducq, D.; Hoang, H.M.; Fournaison, L.; Pateau, O.; Ballot-Miguet, B.; Delahaye, A. Experimental investigation of the use of PCM in an open display cabinet for energy management purposes. *Energy Convers. Manag.* **2019**, *198*. [CrossRef]
154. Xu, X.F.; Zhang, X.L.; Zhou, S.X.; Wang, Y.H.; Liu, L.; Liu, S. Design and Experimental Study on the Storage Type Insulation Box with Multi-temperature. *J. Refrig.* **2019**, *40*, 92–98.
155. Mousazade, A.; Rafee, R.; Valipour, M.S. Thermal performance of cold panels with phase change materials in a refrigerated truck. *Int. J. Refrig.* **2020**, *120*, 119–126. [CrossRef]
156. Ghorbani, B.; Mehrpooya, M. Concentrated solar energy system and cold thermal energy storage (process development and energy analysis). *Sustain. Energy Technol. Assess.* **2019**, *37*, 100607. [CrossRef]
157. Oró, E.; Cabeza, L.F.; Farid, M.M. Experimental and numerical analysis of a chilly bin incorporating phase change material. *Appl. Therm. Eng.* **2013**, *58*, 61–67. [CrossRef]
158. Oró, E.; Gracia, A.D.; Cabeza, L.F. Active phase change material package for thermal protection of ice cream containers. *Int. J. Refrig.* **2013**, *36*, 102–109. [CrossRef]
159. Leducq, D.; Ndoye, F.T.; Alvarez, G. Phase change material for the thermal protection of ice cream during storage and transportation. *Int. J. Refrig.* **2015**, *52*, 133–139. [CrossRef]
160. Liu, M.; Saman, W.; Bruno, F. Development of a novel refrigeration system for refrigerated trucks incorporating phase change material. *Appl. Energy* **2012**, *92*, 336–342. [CrossRef]
161. Liu, M.; Saman, W.; Bruno, F. Computer simulation with TRNSYS for a mobile refrigeration system incorporating a phase change thermal storage unit. *Appl. Energy* **2014**, *132*, 226–235. [CrossRef]
162. Alzuwaid, F.A.; Ge, Y.T.; Tassou, S.A.; Sun, J. The novel use of phase change materials in an open type refrigerated display cabinet: A theoretical investigation. *Appl. Energy* **2016**, *180*, 76–85. [CrossRef]
163. Lu, Y.L.; Zhang, W.H.; Yuan, P.; Xue, M.D.; Qu, Z.G.; Tao, W.Q. Experimental study of heat transfer intensification by using a novel combined shelf in food refrigerated display cabinets (Experimental study of a novel cabinets). *Appl. Therm. Eng.* **2010**, *30*, 85–91. [CrossRef]
164. Alzuwaid, F.; Ge, Y.T.; Tassou, S.A.; Raeisi, A.; Gowreesunker, L. The novel use of phase change materials in a refrigerated display cabinet: An experimental investigation. *Appl. Therm. Eng.* **2015**, *75*, 770–778. [CrossRef]
165. Verpe, E.H.; Tolstorebrov, I.; Sevault, A. Cold thermal energy storage with low-temperature plate freezing of fish on offshore vessels. In Proceedings of the 25th IIR International Congress of Refrigeration, Montréal, QC, Canada, 24–30 August 2019.
166. Selvnes, H.; Hafner, A.; Kauko, H. Cold Thermal Energy Storage Integration in A Large Industrial Refrigeration System. In Proceedings of the 13th IIR—Gustav Lorentzen Conference on Natural Refrigerants, Valencia, Spain, 18–20 June 2018.
167. Hafner, A.; Nordtvedt, T.S.; Rumpf, I. Energy saving potential in freezing applications by applying cold thermal energy storage with solid carbon dioxide. *Procedia Food Sci.* **2011**, *1*, 448–454. [CrossRef]
168. Xiaofeng, X.; Xuelai, Z.; Munyalo, J.M. Simulation Study on Temperature Field and Cold Plate Melting of Cold Storage Refrigerator Car. *Energy Procedia* **2017**, *142*, 3394–3400. [CrossRef]
169. Liu, M.; Saman, W.; Bruno, F. Validation of a mathematical model for encapsulated phase change material flat slabs for cooling applications. *Appl. Therm. Eng.* **2011**, *31*, 2340–2347. [CrossRef]
170. Friend, M.; Stone, S. Challenging requirements in resource challenged environment on a time challenged schedule: A technical solution to support the cold chain for the VSV-Zebov (Merck) Ebola vaccine in Sierra Leone Guinea. In Proceedings of the 2015 IEEE Global Humanitarian Technology Conference, Seattle, WA, USA, 8–11 October 2015.
171. Cheng, W.L.; Ding, M.; Yuan, X.D.; Han, B.C. Analysis of energy saving performance for household refrigerator with thermal storage of condenser and evaporator. *Energy Convers. Manag.* **2017**, *132*, 180–188. [CrossRef]
172. Oró, E.; Miró, L.; Farid, M.M.; Cabeza, L.F. Thermal analysis of a low temperature storage unit using phase change materials without refrigeration system. *Int. J. Refrig.* **2012**, *35*, 1709–1714. [CrossRef]
173. Gin, B.; Farid, M.M. The use of PCM panels to improve storage condition of frozen food. *J. Food Eng.* **2010**, *100*, 372–376. [CrossRef]
174. Zarajabad, O.G.; Ahmadi, R.; Ghaffari, S. Numerical Investigation of Cold Thermal Energy Storage Using Phase Change Material in Freezer. *Eur. J. Eng. Res. Sci.* **2017**, *2*, 1. [CrossRef]
175. Williams, B.G.; Batty, J.C. *ICE (Integrated Cooler Experiment) for COOLSAT*; Springer: Boston, MA, USA, 1995.
176. Wang, Z.; Zhang, Z.; Jia, L.; Yang, L. Paraffin and paraffin/aluminum foam composite phase change material heat storage experimental study based on thermal management of Li-ion battery. *Appl. Therm. Eng.* **2015**, *78*, 428–436. [CrossRef]
177. Heyhata, M.M.; Mousavi, S.; Siavashi, M. Battery thermal management with thermal energy storage composites of PCM, metal foam, fin and nanoparticle. *J. Energy Storage* **2020**, *28*, 101235. [CrossRef]
178. Babapoor, A.; Azizi, M.; Karimi, G. Thermal management of a Li-ion battery using carbon fiber-PCM composites. *Appl. Therm. Eng.* **2015**, *82*, 281–290. [CrossRef]

179. Arshad, A.; Ali, H.M.; Khushnood, S.; Jabbal, M. Experimental investigation of PCM based round pin-fin heat sinks for thermal management of electronics: Effect of pin-fin diameter. *Int. J. Heat Mass Transf.* **2018**, *117*, 861–872. [CrossRef]
180. Alshaer, W.G.; Nada, S.A.; Rady, M.A.; Barrio, E.P.D.; Sommier, A. Thermal management of electronic devices using carbon foam and PCM/nano-composite. *Int. J. Therm. Sci.* **2015**, *89*, 79–86. [CrossRef]
181. Alshaer, W.G.; Nada, S.A.; Rady, M.A.; Bot, C.L.; Barrio, E.P.D. Numerical investigations of using carbon foam/PCM/Nano carbon tubes composites in thermal management of electronic equipment. *Energy Convers. Manag.* **2015**, *89*, 873–884. [CrossRef]
182. Jiang, G.; Huang, J.; Fu, Y.; Cao, M.; Liu, M. Thermal optimization of composite phase change material/expanded graphite for Li-ion battery thermal management. *Appl. Therm. Eng.* **2016**, *108*, 1119–1125. [CrossRef]
183. Sun, X.; Zhang, Q.; Medina, M.A.; Liu, Y.; Liao, S. A study on the use of phase change materials (PCMs) in combination with a natural cold source for space cooling in telecommunications base stations (TBSs) in China. *Appl. Energy* **2014**, *117*, 95–103. [CrossRef]
184. Yantong, L.; Quan, Z.; Xiaoqin, S.; Yaxing, D.; Shuguang, L. Optimization on Performance of the Latent Heat Storage Unit (LHSU) in Telecommunications Base Stations (TBSs) in China. *Energy Procedia* **2015**, *75*, 2119–2124. [CrossRef]
185. Wang, Z.B.; Xiong, W.; Liu, Y.W.; Jiang, C.Y.; Zhu, C.Y. Energy saving research of heat pipe-cool storage air conditioning system used in internet data center. *Refrig. Air-Cond.* **2015**, *15*, 71–74.
186. Chen, X.; Zhang, Q.; Zhai, Z.J.; Wu, D.; Liao, S. Experimental study on operation characteristics of a novel refrigeration system using phase change material. *Energy Build.* **2017**, *150*, 516–526. [CrossRef]
187. Sundaram, A.S.; Seeniraj, R.V.; Velraj, R. An experimental investigation on passive cooling system comprising phase change material and two-phase closed thermosyphon for telecom shelters in tropical and desert regions. *Energy Build.* **2010**, *42*, 1726–1735. [CrossRef]
188. Otsuka, T. Evolution of an LNG terminal: Senboku terminal of Osaka GAS. In Proceedings of the 23rd World Gas Conference, Amsterdam, The Netherlands, 5–9 June 2006; pp. 1362–1372.
189. Zhao, L.; Dong, H.; Tang, J.; Cai, J. Cold energy utilization of liquefied natural gas for capturing carbon dioxide in the flue gas from the magnesite processing industry. *Energy* **2016**, *105*, 45–56. [CrossRef]
190. Al-Musleh, E.I.; Mallapragada, D.S.; Agrawal, R. Efficient electrochemical refrigeration power plant using natural gas with 100% CO2 capture. *J. Power Sources* **2015**, *274*, 130–141. [CrossRef]
191. Na, Z.; Lior, N.; Meng, L.; Wei, H. COOLCEP (cool clean efficient power): A novel CO2-capturing oxy-fuel power system with LNG (liquefied natural gas) coldness energy utilization. *Energy* **2010**, *35*, 1200–1210.
192. Kim, Y.M.; Gil Shin, D.; Kim, C.G. On-Board Cold Thermal Energy Storage System for Hydrogen Fueling Process. *Energies* **2019**, *12*, 561. [CrossRef]
193. Zhang, X.; Li, Z.; Luo, L.; Fan, Y.; Du, Z. A review on thermal management of lithium-ion batteries for electric vehicles. *Energy* **2021**, *238*, 121652. [CrossRef]